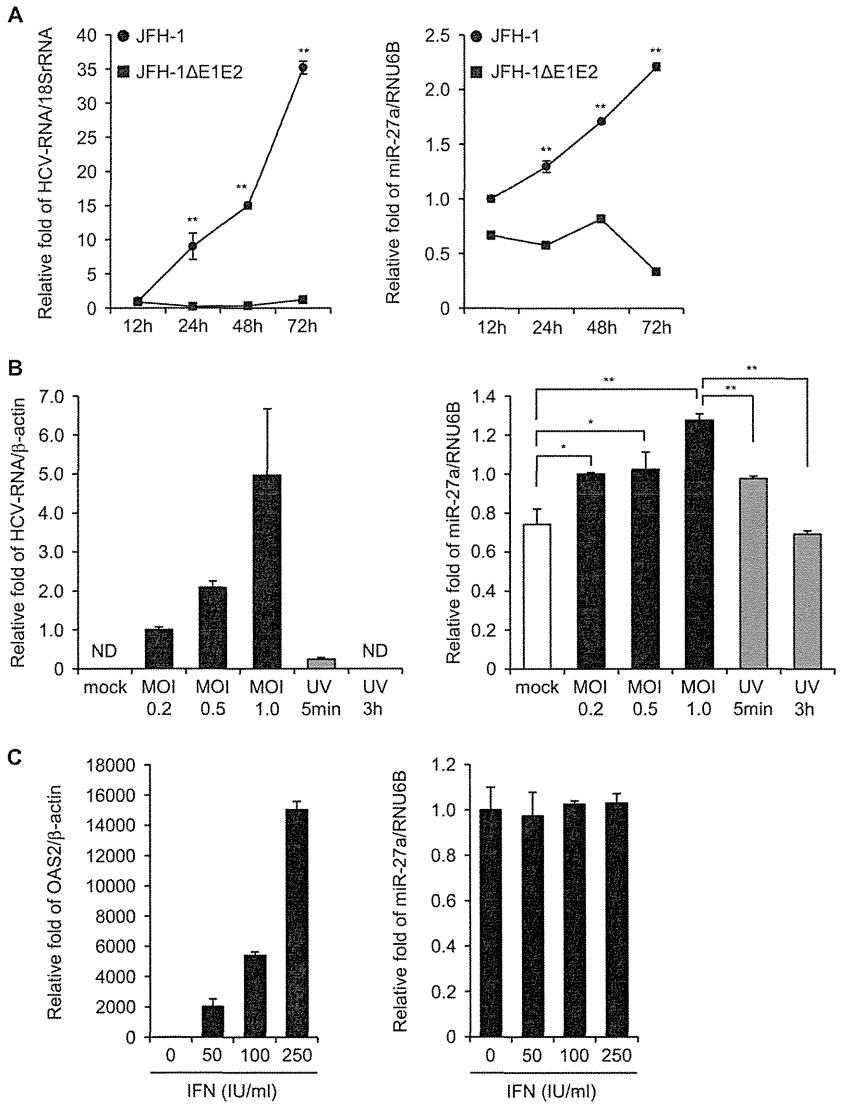

FIG 9 miR-27a is upregulated by HCV infection. (A) Kinetics of HCV replication and induction of miR-27a. Huh-7.5 cells were transfected with JFH-1 RNA or infection-incompetent JFH-1ΔE1E2 RNA (20). At 12, 24, 48, and 72 h posttransfection, HCV RNA (left) and miR-27a (right) levels were quantified by RTD-PCR ($n = 6$). (B) Induction of miR-27a and UV-irradiated HCV particles. Huh-7.5 cells were infected with infectious HCV (multiplicity of infection [MOI] of 0.2, 0.5, or 1) or UV-inactivated HCV. At 72 h postinfection, HCV RNA (left) and miR-27a (right) were quantified by RTD-PCR ($n = 6$). *, $P < 0.01$; **, $P < 0.005$; ND, not detected. (C) Induction of miR-27a and IFN-α treatment. Huh-7.5 cells were treated with different doses of IFN-α. At 24 h posttreatment, OAS2 (left) and miR-27a (right) were quantified by RTD-PCR ($n = 6$). All experiments were performed in duplicate and repeated three times. Values are means ± standard errors.

Several reports have demonstrated the importance of apolipoproteins, including the major components of VLDL and LDL apoE3 (36) and apoB100 (11), in the production of infectious HCV particles. More recently, the functional relevance of ApoA1 in HCV replication and particle production has been reported (37). Here the expression of apoA1, apoB100, and apoE3 was repressed by pre-miR-27a and increased by anti-miR-27a, suggesting that miR-27a regulates the expression of apolipoproteins to reduce the production of infectious HCV particles (Fig. 8F).

Regulation of miR-27a expression through C/EBPα. miR-27a forms a gene cluster with miR-23a and miR-24-2, and both of these miRNAs are regulated by the same promoter (38). However, no detailed analysis of the regulation of this promoter has been carried out. Because the expression of miR-27a was upregulated more in CH-C liver than CH-B liver, it could be speculated that HCV infection induces the expression of miR-27a. To examine this, we evaluated the expression of miR-27a during HCV infection (Fig. 9). The expression of miR-27a increased, correlating with the increase in JFH-1 RNA, while infection-incompetent JFH-1ΔE1E2 did not induce miR-27a expression (Fig. 9A). In addition, UV-irradiated HCV particles did not induce miR-27a expression (Fig. 9B). However, IFN-α treatment did not induce the expression of miR-27a (Fig. 9C). Thus, HCV infection was essential for induction of miR-27a expression.

We identified a C/EBPα binding site (−614 to −606), a key regulator of adipocyte differentiation, in the promoter region of miR-27a. Interestingly, H77Sv2 Gluc2A and tunicamycin

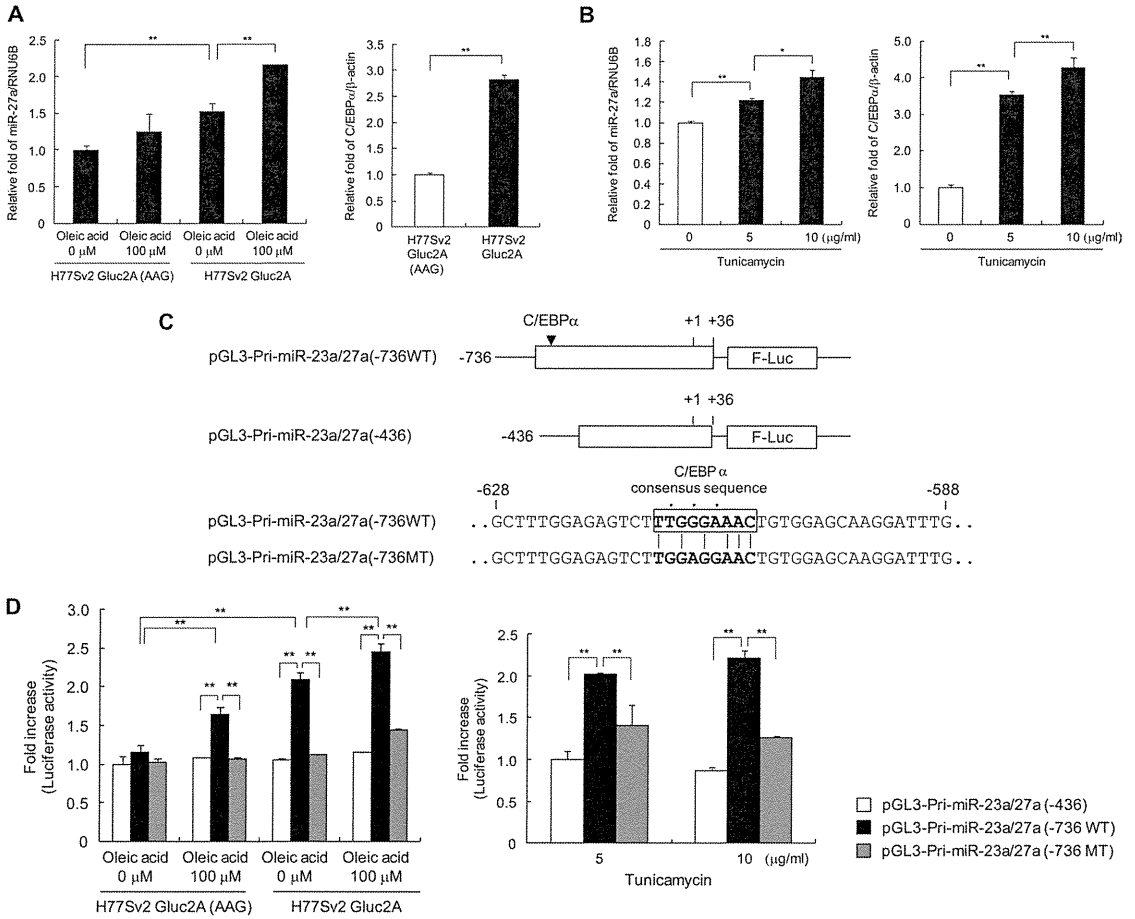

FIG 10 miR-27a is regulated by the adipocyte differentiation factor C/EBPα. (A) Induction of miR-27a and C/EBPα expression by oleic acid and HCV replication. Huh-7.5 cells were transfected with H77Sv2 Gluc2A RNA or H77Sv2 Gluc2A (AAG) RNA. At 24 h posttransfection, oleic acid (100 μM) was added to the culture medium. At 72 h after oleic acid treatment, miR-27a (left) and C/EBPα (right) levels were quantified by RTD-PCR ($n = 6$). (B) Induction of miR-27a and C/EBPα expression by tunicamycin. Huh-7.5 cells were treated with different doses of tunicamycin. At 24 h after tunicamycin treatment, miR-27a (left) and C/EBPα (right) levels were quantified by RTD-PCR ($n = 6$). (C) miR-27a promoter luciferase constructs. pGL3-Pri-miR-23a/27a(−736WT) includes −700 to +36 bp relative to the transcription initiation site of pri-miR-23a~27a~24-2. pGL3-Pri-miR-23a/27a (−436) includes −400 to +36 bp relative to the transcription initiation site of pri-miR-23a~27a~24-2, which lacks the consensus C/EBPα binding site. pGL3-Pri-miR-23a/27a(−736MT) has mutations at the −736WT C/EBPα binding site. (D) miR-27a promoter activity in Huh-7.5 cells following HCV infection and oleic acid (left) or tunicamycin (right) treatment. Reporter constructs lacking the C/EBPα binding site did not respond to any of these conditions ($n = 6$). All experiments were performed in duplicate and repeated three times. Values are means ± standard errors. *, $P < 0.01$; **, $P < 0.005$.

significantly induced the expression of miR-27a and C/EBPα (Fig. 10A and B). To analyze the induction of miR-27a through C/EBPα, we constructed a Luc reporter construct that included the upstream promoter region (−736) of miR-27a [pGL3-Pri-miR-23a/27a(−736WT)] together with a short promoter construct (−436) lacking the C/EBPα binding site [pGL3-Pri-miR-23a/27a(−436)]. In addition, three nucleotide mutations were introduced into the C/EBPα consensus binding site to construct pGL3-Pri-miR-23a/27a(−736MT) (Fig. 10C). The activity of pGL3-Pri-miR-23a/27a(−736WT), but not that of pGL3-Pri-miR-23a/27a(−736MT) or pGL3-Pri-miR-23a/27a(−436), which both lack a C/EBPα binding site, was induced by HCV replication, lipid overload, and tunicamycin treatment (Fig. 10D). These results indicate that the regulation of miR-27a by HCV replication, lipid overload, and ER stress is mediated through C/EBPα.

Pre-miR-27a enhances IFN signaling through the reduction of lipid storage. Finally, we assessed whether miR-27a influences IFN signaling. IFN-α treatment stimulated IFN signaling in a dose-dependent manner by increasing p-STAT1 expression in Huh-7.5 cells (Fig. 11A). Oleic acid impaired this induction of p-STAT1, while pre-miR-27a restored the expression of p-STAT1 and anti-miR-27a impaired this induction by oleic acid. These findings were observed in both HCV-replicating and non-HCV-replicating cells (Fig. 11A).

HCV replication deduced from Gluc activity is shown in Fig. 11B. IFN sensitivity could be estimated by the relative fold changes in Gluc activity from the baseline activity (in the absence of IFN). The results demonstrated that oleic acid reduced IFN sensitivity, while pre-miR-27a increased IFN sensitivity under either condition with or without oleic acid (Fig. 11B).

These findings were further studied with clinical samples. The expression of miR-27a was evaluated in liver biopsy specimens obtained from 41 patients who received pegylated IFN (Peg-IFN) and ribavirin (RBV) combination therapy (Fig. 12A). Interestingly, the expression of miR-27a was significantly higher

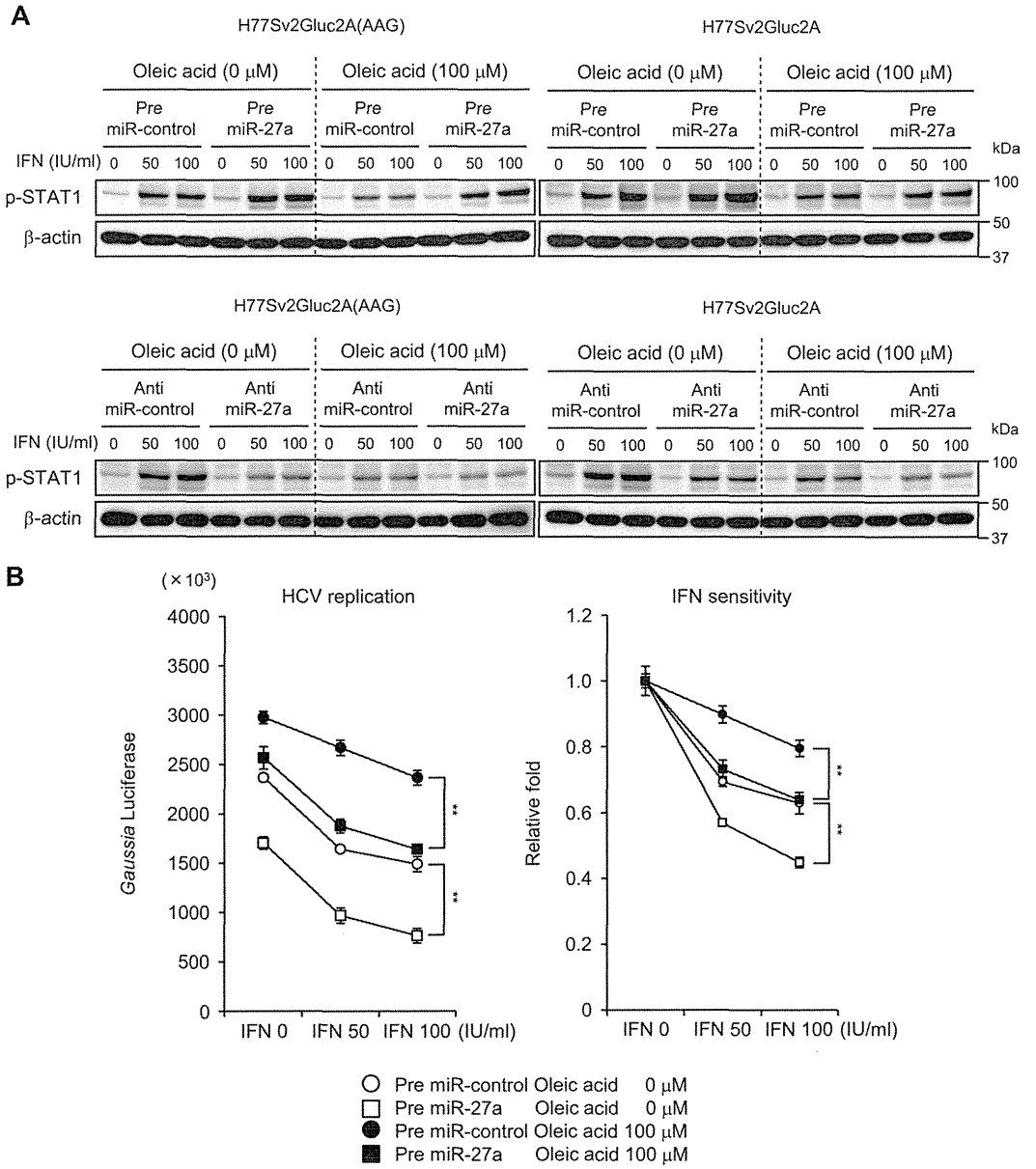

FIG 11 miR-27a restores IFN signaling impaired by lipid overload. (A) Induction of p-STAT1 expression by miR-27a. Huh-7.5 cells were transfected with H77Sv2 Gluc2A RNA or H77Sv2 Gluc2A (AAG) RNA and pre- or anti-miR-control or pre- or anti-miR-27a. At 24 h posttransfection, oleic acid (100 μM) was added to the culture medium. At 48 h after oleic acid treatment, the cells were treated with different doses of IFN-α. At 24 h after IFN treatment, p-STAT1 expression levels were determined by Western blotting. Experiments were repeated three times. (B) Absolute values of Gluc activity (left) and *n*-fold changes in Gluc activity (right) indicate IFN sensitivity ($n = 6$). Experiments were performed in duplicate and repeated three times. Values are means ± standard errors. *, $P < 0.01$; **, $P < 0.005$.

in patients with severe steatosis (grade 3 or 4) than in those with mild steatosis (grade 1 or 2) (Fig. 12B). Importantly, patients with a favorable response to treatment (sustained virological response or transient response) expressed higher miR-27a levels than patients with a poor response (nonresponse) (Fig. 12C). Although there was no significant difference in miR-27a expression according to the interleukin-28B (IL-28B) genotype (Fig. 12D and E), 17 patients had a treatment-resistant IL-28 genotype (TG at rs8099917) (39–41) and 6 of these with a favorable response to treatment expressed significantly higher miR-27a levels than the 11 with a poor response (Fig. 12E). These data suggest that miR-27a enhances IFN signaling and increases the response to IFN treatment.

DISCUSSION

Previously, we examined miRNA expression in HCC and noncancerous background liver tissue infected with HBV and HCV and showed the presence of infection-specific miRNAs that were differentially expressed according to HBV or HCV infection, but not according to the presence of HCC (2). In this study, we pursued the functional analysis of these miRNAs. Among 19 infection-specific miRNAs, we first focused on 6 that were upregulated by

A

No.	Age	Sex	Histological stage			Treatment response			IL28B SNP	
		M:F	F1	F2	F3	SVR	TR	NR	TT	TG
41	54.9±11.2	22:19	15	15	11	17	9	15	24	17

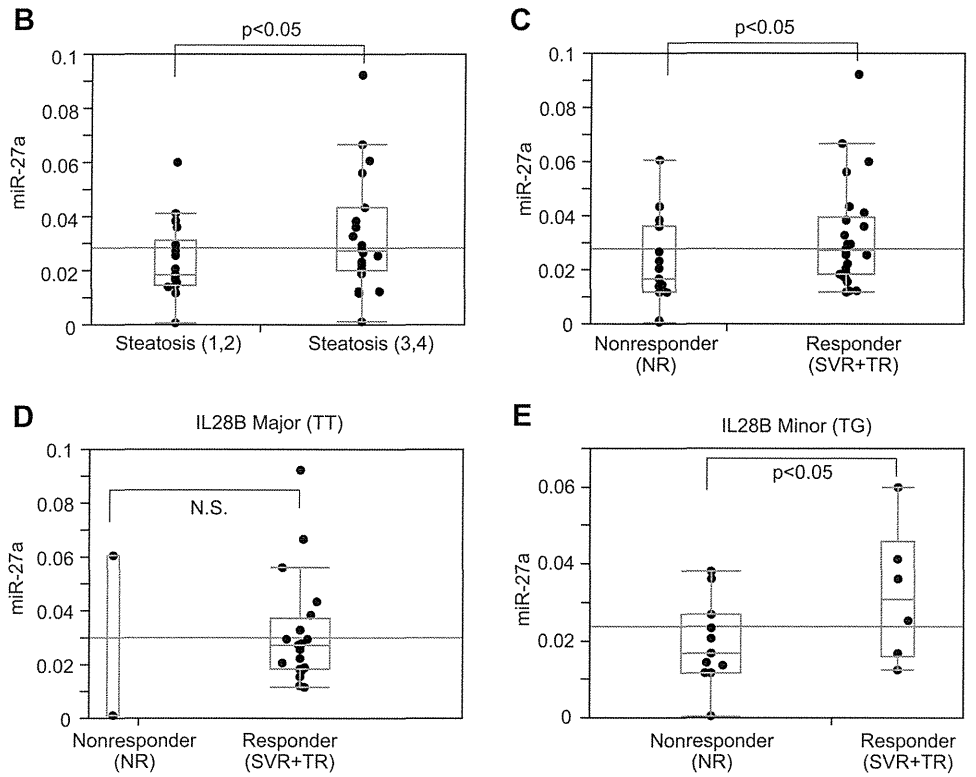

FIG 12 Expression of miR-27a in clinical samples. (A) Clinical characteristics of 41 patients who received Peg-IFN and RBV combination therapy. M:F, male/female ratio; SVR, sustained virological response; TR, transient response; NR, nonresponse; SNP, single nucleotide polymorphism. (B) Significant upregulation of miR-27a expression in the livers of patients with severe steatosis. Steatosis grades 1 and 2, $n = 19$; steatosis grades 3 and 4, $n = 22$. (C) Significant upregulation of miR-27a expression in the livers of patients with a favorable response to treatment (SVR or TR). Nonresponders; $n = 15$; responders, $n = 26$. (D) No significant difference in miR-27a expression between nonresponders and responders of the IL-28B major genotype (treatment-sensitive genotype) was observed. Nonresponders, $n = 3$; responders, $n = 21$. N.S., not significant. (E) Significant upregulation of liver miR-27a was observed in responders of the IL-28B minor genotype (treatment-resistant genotype). Nonresponders, $n = 11$; responders, $n = 6$.

HCV infection, as they were expected to have a positive role in HCV replication. However, inhibition experiments with a series of specific anti-miRNAs showed an unexpected increased in HCV replication. Closer examination clarified that miR-27a had a negative effect on HCV replication. Interestingly, profiling of gene expression in Huh-7.5 cells in which miR-27a was inhibited or overexpressed showed that miR-27a could target lipid metabolism signaling pathways. In support of these findings, the lipid content (TG and TCHO) of Huh-7.5 cells was significantly increased by anti-miR-27a and repressed by pre-miR-27a (Fig. 2 and 3). More importantly, miR-27a was involved in HCV particle formation, as demonstrated by iodixanol gradient centrifugation (Fig. 4). Anti-miR-27a reduced the buoyant density of HCV particles and increased HCV replication and infectivity, while pre-miR-27a decreased HCV replication and dramatically repressed HCV infectivity. In the buoyant-density experiment, the infectious HCV peaks were identical to the RNA peak and the lower infectious virus peak was not observed. We cannot explain this discrepancy from other studies; however, the method used to purify the virus particles could be one reason.

miR-27a regulated many lipid metabolism-related transcription factors, such as RXRα, PPARα, PPARγ, FASN, SREBP1, and SREBP2 (Fig. 5 and 6). We also confirmed that miR-27a targets RXRα in human Huh-7.5 cells, which is concordant with a previous study showing that miR-27a targets RXRα in rat hepatic stellate cells (32). Moreover, we newly demonstrated that the gene for the lipid transporter ABCA1 is a target of miR-27a. ABCA1 mediates the efflux of TCHO and phospholipids to the lipid-poor apolipoproteins ApoA1 and ApoE, which then form nascent HDLs (34, 35). It also mediates the transport of lipids between the Golgi apparatus and the cell membrane. Recently, the knockdown of ABCA1 in rat hepatoma cells increased TG secretion to the culture medium and decreased the cellular levels of FFA (29), while liver-specific ABCA1 knockout mice fed a high-fat diet showed increased plasma TG concentrations and decreased TG and TCHO contents in the liver (42). Thus, ABCA1 regulates the lipid content

of hepatocytes, as well as HDL synthesis. In this study, we confirmed that the repression of ABCA1 decreased cellular TG and TCHO levels in Huh-7.5 cells and, importantly, decreased HCV replication and strikingly repressed HCV infection (Fig. 8).

LXR/RXRα was previously shown to activate the ABCA1 promoter (34), but we clearly demonstrated here that miR-27a directly targets ABCA1. Pre-miR-27a repressed the Luc activity of a reporter construct fused with the ABCA1 3′ UTR, while anti-miR-27a increased it. We also found that miR-27a regulates the expression of ABCA1 in a 3′ UTR sequence-specific manner, as a series of mutations introduced into putative miR-27a binding sites abrogated its regulation (Fig. 7). In addition to these findings, we showed that miR-27a repressed the expression of the apolipoproteins ApoA1, ApoB100, and ApoE3, which were recently shown to play important roles in the production and formation of infectious HCV particles (Fig. 8) (11, 36, 37). Thus, miR-27a may regulate lipid metabolism by reducing lipid synthesis and increasing lipid secretion from cells.

As the expression of miR-27a was upregulated more in CH-C liver than in CH-B liver, it is speculated that miR-27a expression is induced by HCV infection. Indeed, we clearly demonstrated that miR-27a expression was induced by HCV infection, lipid overload, and tunicamycin-induced ER stress (Fig. 9). Furthermore, the adipocyte differentiation-related transcription factor C/EBPα was involved in this regulation. A central role for C/EBPα in the development of adipose tissue has been suggested, as it was found to be sufficient to trigger the differentiation of preadipocytes into mature adipocytes (43). Thus, HCV infection might trigger lipogenesis in hepatocytes by inducing C/EBPα, as shown in this study. Conversely, the induction of C/EBPα expression by miR-27a had a negative effect on lipogenesis and HCV replication. Therefore, miR-27a might play a negative feedback role in HCV infection-induced lipid storage in hepatocytes. Moreover, HCV replication might be hampered by HCV-induced miR-27a, which would partially explain the low HCV titer in CH-C liver.

Besides the anti-HCV effect of miR-27a observed in this study, an antivirus effect against murine cytomegalovirus (MCMV) infection was observed previously (44, 45). MCMV replication was initiated by miR-27a degradation from a viral transcript, while miR-27a had a negative effect on MCMV replication. It was also reported that miR-27a was the target of *Herpesvirus saimiri* U-rich RNAs and was downregulated in transformed T lymphocytes (46). Therefore, the functional relevance of miR-27a in transformed T cells should be explored in a future study. In this study, miR-27a was upregulated by HCV infection, which is in sharp contrast to MCMV and *H. saimiri* infection. Therefore, the differences in antiviral action and host cell interactions also need to be explored further.

Our assessment of miR-27a expression in patients receiving Peg-IFN and RBV combination therapy showed that those with high miR-27a levels had a more favorable treatment response (Fig. 12). Moreover, miR-27a significantly enhanced IFN signaling (Fig. 11), suggesting that it might have therapeutic benefits in combination with IFN therapy, especially in patients with the IFN-resistant IL-28B genotype, who show a more severe steatosis than those with the IFN-sensitive IL-28B genotype (39–41). Further studies should be performed to confirm these findings with more clinical samples.

Although miR-27a has been shown to be upregulated in cancers of the breast, kidney, ovary, and gastric region, its downregulation has been reported in colorectal cancer, malignant melanoma, oral squamous cell carcinoma, and acute promyelocytic leukemia (47). However, its importance in HCC remains controversial, with one report observing its upregulation compared with the level in normal liver tissue (48), while another showed lower miR-27a expression in HCC than in paired nontumor tissues (49). Moreover, our previous findings on HBV-related and HCV-related HCC showed no miR-27a upregulation compared with the level in the paired background liver (1.14-fold, $P = 0.49$).

In summary, we have revealed the important role of miR-27a in HCV replication for the first time. These findings will be applicable in the improvement of the therapeutic effects of anti-HCV therapy, especially in patients showing treatment resistance and severe hepatic steatosis.

ACKNOWLEDGMENTS

We thank Mina Nishiyama and Masayo Baba for their excellent technical assistance.

We have no potential competing interests to declare.

REFERENCES

1. **Esteller M.** 2011. Non-coding RNAs in human disease. Nat. Rev. Genet. 12:861–874.
2. **Ura S, Honda M, Yamashita T, Ueda T, Takatori H, Nishino R, Sunakozaka H, Sakai Y, Horimoto K, Kaneko S.** 2009. Differential microRNA expression between hepatitis B and hepatitis C leading disease progression to hepatocellular carcinoma. Hepatology 49:1098–1112.
3. **André P, Komurian-Pradel F, Deforges S, Perret M, Berland JL, Sodoyer M, Pol S, Brechot C, Paranhos-Baccala G, Lotteau V.** 2002. Characterization of low- and very-low-density hepatitis C virus RNA-containing particles. J. Virol. 76:6919–6928.
4. **Thomssen R, Bonk S, Propfe C, Heermann KH, Kochel HG, Uy A.** 1992. Association of hepatitis C virus in human sera with beta-lipoprotein. Med. Microbiol. Immunol. 181:293–300.
5. **Thomssen R, Bonk S, Thiele A.** 1993. Density heterogeneities of hepatitis C virus in human sera due to the binding of beta-lipoproteins and immunoglobulins. Med. Microbiol. Immunol. 182:329–334.
6. **Agnello V, Abel G, Elfahal M, Knight GB, Zhang QX.** 1999. Hepatitis C virus and other Flaviviridae viruses enter cells via low density lipoprotein receptor. Proc. Natl. Acad. Sci. U. S. A. 96:12766–12771.
7. **Germi R, Crance JM, Garin D, Guimet J, Lortat-Jacob H, Ruigrok RW, Zarski JP, Drouet E.** 2002. Cellular glycosaminoglycans and low density lipoprotein receptor are involved in hepatitis C virus adsorption. J. Med. Virol. 68:206–215.
8. **Triyatni M, Saunier B, Maruvada P, Davis AR, Ulianich L, Heller T, Patel A, Kohn LD, Liang TJ.** 2002. Interaction of hepatitis C virus-like particles and cells: a model system for studying viral binding and entry. J. Virol. 76:9335–9344.
9. **Shi ST, Lee KJ, Aizaki H, Hwang SB, Lai MM.** 2003. Hepatitis C virus RNA replication occurs on a detergent-resistant membrane that cofractionates with caveolin-2. J. Virol. 77:4160–4168.
10. **Miyanari Y, Atsuzawa K, Usuda N, Watashi K, Hishiki T, Zayas M, Bartenschlager R, Wakita T, Hijikata M, Shimotohno K.** 2007. The lipid droplet is an important organelle for hepatitis C virus production. Nat. Cell Biol. 9:1089–1097.
11. **Huang H, Sun F, Owen DM, Li W, Chen Y, Gale M, Jr, Ye J.** 2007. Hepatitis C virus production by human hepatocytes dependent on assembly and secretion of very low-density lipoproteins. Proc. Natl. Acad. Sci. U. S. A. 104:5848–5853.
12. **Bressler BL, Guindi M, Tomlinson G, Heathcote J.** 2003. High body mass index is an independent risk factor for nonresponse to antiviral treatment in chronic hepatitis C. Hepatology 38:639–644.
13. **Poynard T, Ratziu V, McHutchison J, Manns M, Goodman Z, Zeuzem S, Younossi Z, Albrecht J.** 2003. Effect of treatment with peginterferon or interferon alfa-2b and ribavirin on steatosis in patients infected with hepatitis C. Hepatology 38:75–85.

14. Jopling CL, Yi M, Lancaster AM, Lemon SM, Sarnow P. 2005. Modulation of hepatitis C virus RNA abundance by a liver-specific MicroRNA. Science 309:1577–1581.
15. Murakami Y, Aly HH, Tajima A, Inoue I, Shimotohno K. 2009. Regulation of the hepatitis C virus genome replication by miR-199a. J. Hepatol. 50:453–460.
16. Hou W, Tian Q, Zheng J, Bonkovsky HL. 2010. MicroRNA-196 represses Bach1 protein and hepatitis C virus gene expression in human hepatoma cells expressing hepatitis C viral proteins. Hepatology 51:1494–1504.
17. Bandyopadhyay S, Friedman RC, Marquez RT, Keck K, Kong B, Icardi MS, Brown KE, Burge CB, Schmidt WN, Wang Y, McCaffrey AP. 2011. Hepatitis C virus infection and hepatic stellate cell activation downregulate miR-29: miR-29 overexpression reduces hepatitis C viral abundance in culture. J. Infect. Dis. 203:1753–1762.
18. Cheng JC, Yeh YJ, Tseng CP, Hsu SD, Chang YL, Sakamoto N, Huang HD. 2012. Let-7b is a novel regulator of hepatitis C virus replication. Cell. Mol. Life Sci. 69:2621–2633.
19. Bhanja Chowdhury J, Shrivastava S, Steele R, Di Bisceglie AM, Ray R, Ray RB. 2012. Hepatitis C virus infection modulates expression of interferon stimulatory gene IFITM1 by upregulating miR-130A. J. Virol. 86:10221–10225.
20. Wakita T, Pietschmann T, Kato T, Date T, Miyamoto M, Zhao Z, Murthy K, Habermann A, Kräusslich HG, Mizokami M, Bartenschlager R, Liang TJ. 2005. Production of infectious hepatitis C virus in tissue culture from a cloned viral genome. Nat. Med. 11:791–796.
21. Shetty S, Kim S, Shimakami T, Lemon SM, Mihailescu MR. 2010. Hepatitis C virus genomic RNA dimerization is mediated via a kissing complex intermediate. RNA. 16:913–925.
22. Che ML, Yan YC, Zhang Y, Gu Y, Wang NS, Chen N, Mao PJ, Zhang JY, Ding XQ, Yuan WJ, Mei CL, Yao J, Fan YL, Zhou Y, Zhang W, Zhu HW, Liu M, Jin HM, Qian JQ. 2009. Analysis of drug-induced acute renal failure in Shanghai. Zhonghua Yi Xue Za Zhi 89:744–749. (In Chinese.)
23. Shimakami T, Welsch C, Yamane D, McGivern DR, Yi M, Zeuzem S, Lemon SM. 2011. Protease inhibitor-resistant hepatitis C virus mutants with reduced fitness from impaired production of infectious virus. Gastroenterology 140:667–675.
24. Yi M, Villanueva RA, Thomas DL, Wakita T, Lemon SM. 2006. Production of infectious genotype 1a hepatitis C virus (Hutchinson strain) in cultured human hepatoma cells. Proc. Natl. Acad. Sci. U. S. A. 103:2310–2315.
25. Honda M, Takehana K, Sakai A, Tagata Y, Shirasaki T, Nishitani S, Muramatsu T, Yamashita T, Nakamoto Y, Mizukoshi E, Sakai Y, Nakamura M, Shimakami T, Yi M, Lemon SM, Suzuki T, Wakita T, Kaneko S. 2011. Malnutrition impairs interferon signaling through mTOR and FoxO pathways in patients with chronic hepatitis C. Gastroenterology 141:128–140.
26. Malhi H, Barreyro FJ, Isomoto H, Bronk SF, Gores GJ. 2007. Free fatty acids sensitise hepatocytes to TRAIL mediated cytotoxicity. Gut 56:1124–1131.
27. Honda M, Nakamura M, Tateno M, Sakai A, Shimakami T, Shirasaki T, Yamashita T, Arai K, Sakai Y, Kaneko S. 2010. Differential interferon signaling in liver lobule and portal area cells under treatment for chronic hepatitis C. J. Hepatol. 53:817–826.
28. Shirasaki T, Honda M, Mizuno H, Shimakami T, Okada H, Sakai Y, Murakami S, Wakita T, Kaneko S. 2010. La protein required for internal ribosome entry site-directed translation is a potential therapeutic target for hepatitis C virus replication. J. Infect. Dis. 202:75–85.
29. Chung S, Gebre AK, Seo J, Shelness GS, Parks JS. 2010. A novel role for ABCA1-generated large pre-beta migrating nascent HDL in the regulation of hepatic VLDL triglyceride secretion. J. Lipid Res. 51:729–742.
30. Lewis BP, Burge CB, Bartel DP. 2005. Conserved seed pairing, often flanked by adenosines, indicates that thousands of human genes are microRNA targets. Cell 120:15–20.
31. Lee JS, Mendez R, Heng HH, Yang ZQ, Zhang K. 2012. Pharmacological ER stress promotes hepatic lipogenesis and lipid droplet formation. Am. J. Transl. Res. 4:102–113.
32. Ji J, Zhang J, Huang G, Qian J, Wang X, Mei S. 2009. Over-expressed microRNA-27a and 27b influence fat accumulation and cell proliferation during rat hepatic stellate cell activation. FEBS Lett. 583:759–766.
33. Kim SY, Kim AY, Lee HW, Son YH, Lee GY, Lee JW, Lee YS, Kim JB. 2010. miR-27a is a negative regulator of adipocyte differentiation via suppressing PPARgamma expression. Biochem. Biophys. Res. Commun. 392:323–328.
34. Schmitz G, Langmann T. 2005. Transcriptional regulatory networks in lipid metabolism control ABCA1 expression. Biochim. Biophys. Acta 1735:1–19.
35. Liu M, Chung S, Shelness GS, Parks JS. 2012. Hepatic ABCA1 and VLDL triglyceride production. Biochim. Biophys. Acta 1821:770–777.
36. Hishiki T, Shimizu Y, Tobita R, Sugiyama K, Ogawa K, Funami K, Ohsaki Y, Fujimoto T, Takaku H, Wakita T, Baumert TF, Miyanari Y, Shimotohno K. 2010. Infectivity of hepatitis C virus is influenced by association with apolipoprotein E isoforms. J. Virol. 84:12048–12057.
37. Mancone C, Steindler C, Santangelo L, Simonte G, Vlassi C, Longo MA, D'Offizi G, Di Giacomo C, Pucillo LP, Amicone L, Tripodi M, Alonzi T. 2011. Hepatitis C virus production requires apolipoprotein A-I and affects its association with nascent low-density lipoproteins. Gut 60:378–386.
38. Lee Y, Kim M, Han J, Yeom KH, Lee S, Baek SH, Kim VN. 2004. MicroRNA genes are transcribed by RNA polymerase II. EMBO J. 23:4051–4060.
39. O'Brien TR. 2009. Interferon-alfa, interferon-lambda and hepatitis C. Nat. Genet. 41:1048–1050.
40. Suppiah V, Moldovan M, Ahlenstiel G, Berg T, Weltman M, Abate ML, Bassendine M, Spengler U, Dore GJ, Powell E, Riordan S, Sheridan D, Smedile A, Fragomeli V, Muller T, Bahlo M, Stewart GJ, Booth DR, George J. 2009. IL28B is associated with response to chronic hepatitis C interferon-alpha and ribavirin therapy. Nat. Genet. 41:1100–1104.
41. Tanaka Y, Nishida N, Sugiyama M, Kurosaki M, Matsuura K, Sakamoto N, Nakagawa M, Korenaga M, Hino K, Hige S, Ito Y, Mita E, Tanaka E, Mochida S, Murawaki Y, Honda M, Sakai A, Hiasa Y, Nishiguchi S, Koike A, Sakaida I, Imamura M, Ito K, Yano K, Masaki N, Sugauchi F, Izumi N, Tokunaga K, Mizokami M. 2009. Genome-wide association of IL28B with response to pegylated interferon-alpha and ribavirin therapy for chronic hepatitis C. Nat. Genet. 41:1105–1109.
42. Chung S, Timmins JM, Duong M, Degirolamo C, Rong S, Sawyer JK, Singaraja RR, Hayden MR, Maeda N, Rudel LL, Shelness GS, Parks JS. 2010. Targeted deletion of hepatocyte ABCA1 leads to very low density lipoprotein triglyceride overproduction and low density lipoprotein hypercatabolism. J. Biol. Chem. 285:12197–12209.
43. Porse BT, Pedersen TA, Xu X, Lindberg B, Wewer UM, Friis-Hansen L, Nerlov C. 2001. E2F repression by C/EBPalpha is required for adipogenesis and granulopoiesis in vivo. Cell 107:247–258.
44. Libri V, Helwak A, Miesen P, Santhakumar D, Borger JG, Kudla G, Grey F, Tollervey D, Buck AH. 2012. Murine cytomegalovirus encodes a miR-27 inhibitor disguised as a target. Proc. Natl. Acad. Sci. U. S. A. 109:279–284.
45. Marcinowski L, Tanguy M, Krmpotic A, Radle B, Lisnic VJ, Tuddenham L, Chane-Woon-Ming B, Ruzsics Z, Erhard F, Benkartek C, Babic M, Zimmer R, Trgovcich J, Koszinowski UH, Jonjic S, Pfeffer S, Dolken L. 2012. Degradation of cellular mir-27 by a novel, highly abundant viral transcript is important for efficient virus replication in vivo. PLoS Pathog. 8:e1002510. doi:10.1371/journal.ppat.1002510.
46. Cazalla D, Yario T, Steitz JA. 2010. Down-regulation of a host microRNA by a Herpesvirus saimiri noncoding RNA. Science 328:1563–1566.
47. Chhabra R, Dubey R, Saini N. 2010. Cooperative and individualistic functions of the microRNAs in the miR-23a~27a~24-2 cluster and its implication in human diseases. Mol. Cancer 9:232.
48. Huang S, He X, Ding J, Liang L, Zhao Y, Zhang Z, Yao X, Pan Z, Zhang P, Li J, Wan D, Gu J. 2008. Upregulation of miR-23a approximately 27a approximately 24 decreases transforming growth factor-beta-induced tumor-suppressive activities in human hepatocellular carcinoma cells. Int. J. Cancer 123:972–978.
49. Wang W, Zhao LJ, Tan YX, Ren H, Qi ZT. 2012. MiR-138 induces cell cycle arrest by targeting cyclin D3 in hepatocellular carcinoma. Carcinogenesis 33:1113–1120.

Genomics 101 (2013) 238–248

Contents lists available at SciVerse ScienceDirect

Genomics

journal homepage: www.elsevier.com/locate/ygeno

Gene expression profiling of hepatitis B- and hepatitis C-related hepatocellular carcinoma using graphical Gaussian modeling☆

Teruyuki Ueda [a], Masao Honda [a,b,*], Katsuhisa Horimoto [c], Sachiyo Aburatani [c], Shigeru Saito [c], Taro Yamashita [a], Yoshio Sakai [a], Mikiko Nakamura [a], Hajime Takatori [a], Hajime Sunagozaka [a], Shuichi Kaneko [a]

[a] Department of Gastroenterology, Graduate School of Medicine, Kanazawa University, Kanazawa, Takara-Machi 13-1, Kanazawa 920-8641, Japan
[b] Department of Advanced Medical Technology, Kanazawa University Graduate School of Health Medicine, Kanazawa, Takara-Machi 13-1, Kanazawa 920-8641, Japan
[c] Biological Network Team, Computational Biology Research Center, National Institute of Advanced Industrial Science and Technology, Aomi 2-4-7, Koto-ku, Tokyo 135-0064, Japan

ARTICLE INFO

Article history:
Received 1 October 2012
Accepted 11 February 2013
Available online 26 February 2013

Keywords:
Hepatitis B virus
Hepatitis C virus
Hepatocellular carcinoma
Gene expression

ABSTRACT

Background & aims: Gene expression profiling of hepatocellular carcinoma (HCC) and background liver has been studied extensively; however, the relationship between the gene expression profiles of different lesions has not been assessed.
Methods: We examined the expression profiles of 34 HCC specimens (17 hepatitis B virus [HBV]-related and 17 hepatitis C virus [HCV]-related) and 71 non-tumor liver specimens (36 chronic hepatitis B [CH-B] and 35 chronic hepatitis C [CH-C]) using an in-house cDNA microarray consisting of liver-predominant genes. Graphical Gaussian modeling (GGM) was applied to elucidate the interactions of gene clusters among the HCC and non-tumor lesions.
Results: In CH-B-related HCC, the expression of vascular endothelial growth factor-family signaling and regulation of T cell differentiation, apoptosis, and survival, as well as development-related genes was up-regulated. In CH-C-related HCC, the expression of ectodermal development and cell proliferation, wnt receptor signaling, cell adhesion, and defense response genes was also up-regulated. Many of the metabolism-related genes were down-regulated in both CH-B- and CH-C-related HCC. GGM analysis of the HCC and non-tumor lesions revealed that DNA damage response genes were associated with AP1 signaling in non-tumor lesions, which mediates the expression of many genes in CH-B-related HCC. In contrast, signal transducer and activator of transcription 1 and phosphatase and tensin homolog were associated with early growth response protein 1 signaling in non-tumor lesions, which potentially promotes angiogenesis, fibrogenesis, and tumorigenesis in CH-C-related HCC.
Conclusions: Gene expression profiling of HCC and non-tumor lesions revealed the predisposing changes of gene expression in HCC. This approach has potential for the early diagnosis and possible prevention of HCC.

1. Introduction

Hepatocellular carcinoma (HCC) is one of the most common malignancies worldwide with a particularly poor patient outcome [1]. It often develops as a result of chronic liver disease associated with hepatitis B (HBV) or hepatitis C virus (HCV) infection or with other etiologies such as long-term alcohol abuse, autoimmunity, and hemochromatosis [2]. HBV and HCV infections are the leading cause of HCC in the world [3]. In Japan, approximately 85% of patients with HCC are positive for the HBV surface antigen or anti-HCV antibody. Approximately 7% of patients with HCV-related liver cirrhosis develop HCC [4] and 3% of patients with HBV-related liver cirrhosis develop HCC [5].

Gene expression analysis of HCC has revealed from previous work, the activation of the wnt/β-catenin, pRb, p53, transforming growth factor-β, mitogen-activated protein kinase, and Janus kinase/signal transducer and activator of transcription pathways, stress response signaling, and epidermal growth factor receptor [6–8]. In addition, we have previously reported that the gene expression profiles in the livers of patients with chronic hepatitis B (CH-B) and chronic hepatitis C (CH-C) were different. Pro-apoptotic and DNA repair responses were predominant in CH-B, while inflammatory and anti-apoptotic phenotypes were predominant in CH-C [9,10]. Furthermore, we optimized

Abbreviations: CH-B, chronic hepatitis B; CH-C, chronic hepatitis C; CLL, cells in liver lobules; CPA, cells in the portal area; EF, early fibrosis; EGR1, early growth response protein 1; ESR1, estrogen receptor 1; GGM, graphical Gaussian modeling; HBV, hepatitis B virus; HCC, hepatocellular carcinoma; HCV, hepatitis C virus; hTERT, human telomerase reverse transcriptase; LCM, laser capture microdissection; LF, late fibrosis; PCCM, partial correlation coefficient matrix; PTEN, phosphatase and tensin homolog; SD, standard deviation; SHC, src homology 2 domain containing; STAT1, signal transducer and activator of transcription 1; TCA, tricarboxylic acid cycle; VEGF, vascular endothelial growth factor.

☆ Conflict of interest: The authors declare no conflict of interest.

* Corresponding author at: Department of Gastroenterology, Graduate School of Medicine, Kanazawa University, Takara-Machi 13-1, Kanazawa 920-8641, Japan. Fax: +81 76 234 4250.
E-mail address: mhonda@m-kanazawa.jp (M. Honda).

0888-7543/$ – see front matter © 2013 Elsevier Inc. All rights reserved.
http://dx.doi.org/10.1016/j.ygeno.2013.02.007

the laser capture microdissection (LCM) method to isolate cells in liver lobules (CLL) and cells in the portal area (CPA) for detailed gene expression analysis [10,11]. However, it is still unknown how cancer signaling pathways are activated in HCC. As HCC frequently develops from a cirrhotic liver, analyzing the relationship of signaling pathways between HCC and non-cancerous liver tissue might be a useful approach for revealing the mechanism that ultimately leads to the development of HCC.

Graphical Gaussian modeling (GGM) is utilized widely to infer or test the relationships between multiple variables [12–14]. Previously, we developed a method that combines cluster analysis with GGM to infer a genetic network on the basis of expression profile data. Analysis of the expression profile of *Saccharomyces cerevisiae* revealed a model of its genetic network, and the accuracy of the inferred network was confirmed by its agreement with the cumulative results of experimental studies [15]. Therefore, GGM has the potential to be a useful analytical tool to identify the relationship between the gene expression profiles of HCC and non-cancerous liver tissue.

In the present study, we extended the analysis of gene expression in HCC and applied GGM analysis [15,16]. Indeed, our procedure inferred the relationships between gene groups defined by clustering, and its application enabled us to elucidate the framework of the gene clusters in relation to the hepatocellular carcinogenesis of CH-B and CH-C.

2. Results

2.1. Expressed genes in CH-B-related HCC

The gene expression profiles of whole liver biopsy specimens and surgically resected liver were obtained from 36 patients with CH-B, 17 with CH-B-related HCC, 35 with CH-C, and 17 with CH-C-related HCC. The clinical characteristics of the patients are shown in Supplemental Tables A and B. We categorized the F1 and F2 fibrosis stages as early fibrosis (EF; $n = 13$ for CH-B and $n = 12$ for CH-C) and the F3 and F4 fibrosis stages as late fibrosis (LF; $n = 22$ for CH-B and $n = 23$ for CH-C).

The 783 differentially expressed genes in CH-B-related HCC were identified across 20 clusters, of which 4 (Nos. 8, 9, 11, and 20) were up-regulated and 12 (No. 1–7, 12–14, 16, and 17) were down-regulated (Fig. 1 and Supplemental Table C). The up-regulated clusters were comprised angiogenesis, cell cycle, apoptosis, and survival-related genes. Placental growth factor, vascular endothelial growth factor (VEGF)-related protein, SUMO-activating enzyme subunit 2, cyclin E1, and baculoviral IAP repeat-containing 5 were up-regulated (Nos. 8, 9, and 11). In addition, oncogene-related proteins, such as v-myc myelocytomatosis viral-related oncogene (No. 9), telomerase-associated protein 1, and stathmin 1/oncoprotein 18 (No. 8), tumor marker genes, such glypican 3, and growth factors, such as midkine (No. 9), were also up-regulated. In cluster No. 20, the proliferation and invasiveness-related gene and protein tyrosine kinase 2 were up-regulated.

Down-regulation was prominent in many metabolism-related genes including ornithine aminotransferase, insulin receptor substrate 1, glutamate dehydrogenase 2, acyl-coenzyme A oxidase 2, and acetyl-coenzyme A acyltransferase 2, as well as many cytochrome P450 family genes, suggesting impaired xenobiotic, amino acid, and lipid metabolism (Nos. 6, 7, 12, 13, 16, and 17). The characteristic genes expressed in CH-B-related HCC are shown in Table 1.

2.2. Expressed genes in CH-C-related HCC

The 668 differentially expressed genes in CH-C-related HCC were identified across 18 genetic clusters, of which 5 (Nos. 10, 12, 14, 15, and 18) were up-regulated and 11 (Nos. 1–7, 11, 13, 16, and 17) were down-regulated (Fig. 2 and Supplemental Table D). Cluster No. 12 comprised immune defense response genes, such as chemokine (the C-C motif) ligand 19, natural killer cell transcript 4, major histocompatibility complex class I B, major histocompatibility complex class II DQ beta 1, and ubiquitin-specific protease 8. Cluster No. 14 comprised cytoskeleton-associated, cell cycle, mitosis-related, and MAPKKK cascade-related genes, such as tubulin, src homology 2 domain containing (SHC) transforming protein 1, sterile alpha motif domain containing 9, S100 calcium binding protein A10, annexin A2, cyclin B1, platelet-activating factor acetylhydrolase, isoform Ib, and vimentin. In cluster No. 15, glypican 3, aldo-keto reductase family 1, member B10, ATP citrate lyase, farnesyl diphosphate synthase, serine protease inhibitor, and Kazal type 1 were up-regulated. Cluster No. 15 included many candidate tumor markers of HCC. Interestingly, LCM analysis revealed that many of the up-regulated genes in clusters Nos. 12, 14, and 15 were preferentially expressed in CPA. Cluster No. 18 comprised regulation of G1/S checkpoint, signal transduction, and ectoderm development-related genes, such as bone morphogenetic protein 4, cyclin-dependent kinase inhibitor 2A, fibroblast growth factor 9, and ornithine decarboxylase 1. Similar to CH-B-related HCC, many of the metabolism-related genes, including glucose, lipid, and amino acid genes, were down-regulated. The unique feature of lipid metabolism in CH-C-related HCC was the up-regulation of cholesterol and fatty acid synthesis genes and down-regulation of cholesterol metabolism and β oxidation genes. It was characterized by the up-regulation of stearoyl-CoA desaturase, farnesyl diphosphate synthase (No. 14), and ATP citrate lyase (No. 15), and down-regulation of acetyl-coenzyme A acetyltransferase 1. The characteristic genes expressed in CH-C-related HCC are shown in Table 2. Representative gene expression levels confirmed by TaqMan PCR are shown in Supplemental Fig. C1.

Pathway analysis of the combined up- and down-regulated clusters is shown in Supplemental Fig. D and Supplemental Table E. In CH-C-related HCC, immune response- and cytoskeleton-related genes, such as actin, tubulin, and vimentin, were up-regulated, while in CH-B-related HCC, cell matrix interaction genes, such as collagen IV and matrix metalloproteinase, were up-regulated. Immune-related genes were shown to be down-regulated in both CH-C- and CH-B-related HCC by MetaCore™ database analysis (Thomson Reuters, New York, NY) (Supplemental Fig. D). Gene annotation by DAVID Bioinformatics Resources 6.7 (http://david.abcc.ncifcrf.gov/) [17] showed that oxidative phosphorylation and ATP synthesis coupled electron transport were up-regulated more in CH-C-related HCC than in CH-B-related HCC (Supplemental Table E).

2.3. Expressed genes in CH-B and CH-C

Differentially expressed genes in CH-B or CH-C were identified by backward selection, which did not include genes that were differentially expressed in CH-B- or CH-C-related HCC. As HCC frequently develops in the LF stage of liver disease, gene expression was evaluated in this stage. A total of 352 genes were differentially expressed in the LF stage of CH-B and classified into 21 clusters, of which 7 (Nos. 2, 3, 9, 10, 15, 16, and 18) were up-regulated and 11 (No. 5–7, 8, 11–14, 17, 20, and 21) were down-regulated (Supplemental Fig. B and Supplemental Table F).

In the CH-B fibrotic liver, genes involved in apoptosis, survival, and response to stress, as well as chemokine- and cytokine-related genes and wnt beta-catenin and angiogenesis-related genes, were up-regulated. Interestingly, these genes were already up-regulated in the EF stage of CH-B. In contrast, metabolism-related genes, such as those for pyruvate, cholesterol, and retinol metabolism and the mitochondrial tricarboxylic acid (TCA) cycle, were down-regulated.

In total, 214 genes were differentially expressed in the LF stage of CH-C and classified into 7 gene clusters, of which 1 was up-regulated (No. 1) and 3 were down-regulated (Nos. 3, 5, and 6) (Supplemental Fig. B and Supplemental Table G). In CH-C, genes involved in the interferon signaling pathway, leukocyte chemotaxis, and immune response were preferentially up-regulated. These genes were expressed at a significantly higher level in CPA than in CLL in the liver (No. 1). Conversely, many metabolism and liver function-related genes were down-regulated (Nos. 3, 5, and 6). These genes were expressed at significantly higher levels in CLL compared to CPA in the liver.

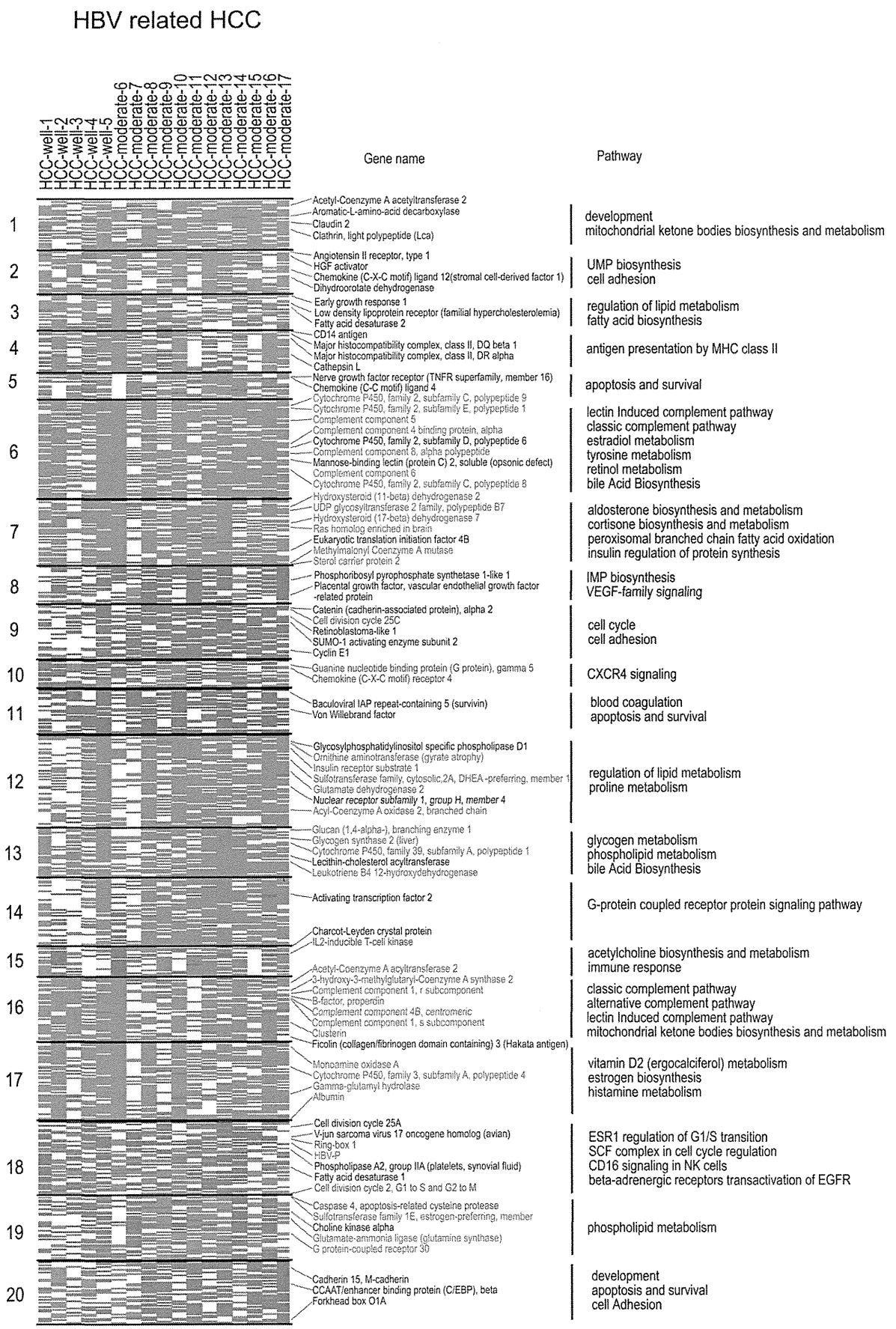
HBV related HCC
HCC-well-1
HCC-well-2
HCC-well-3
HCC-well-4
HCC-well-5
HCC-moderate-6
HCC-moderate-7
HCC-moderate-8
HCC-moderate-9
HCC-moderate-10
HCC-moderate-11
HCC-moderate-12
HCC-moderate-13
HCC-moderate-14
HCC-moderate-15
HCC-moderate-16
HCC-moderate-17
Gene name
Pathway
1
Acetyl-Coenzyme A acetyltransferase 2
Aromatic-L-amino-acid decarboxylase
Claudin 2
Clathrin, light polypeptide (Lca)
development
mitochondrial ketone bodies biosynthesis and metabolism
2
Angiotensin II receptor, type 1
HGF activator
Chemokine (C-X-C motif) ligand 12(stromal cell-derived factor 1)
Dihydroorotate dehydrogenase
UMP biosynthesis
cell adhesion
3
Early growth response 1
Low density lipoprotein receptor (familial hypercholesterolemia)
Fatty acid desaturase 2
regulation of lipid metabolism
fatty acid biosynthesis
4
CD14 antigen
Major histocompatibility complex, class II, DQ beta 1
Major histocompatibility complex, class II, DR alpha
Cathepsin L
antigen presentation by MHC class II
5
Nerve growth factor receptor (TNFR superfamily, member 16)
Chemokine (C-C motif) ligand 4
apoptosis and survival
6
Cytochrome P450, family 2, subfamily C, polypeptide 9
Cytochrome P450, family 2, subfamily E, polypeptide 1
Complement component 5
Complement component 4 binding protein, alpha
Cytochrome P450, family 2, subfamily D, polypeptide 6
Complement component 8, alpha polypeptide
Mannose-binding lectin (protein C) 2, soluble (opsonic defect)
Complement component 6
Cytochrome P450, family 2, subfamily C, polypeptide 8
lectin Induced complement pathway
classic complement pathway
estradiol metabolism
tyrosine metabolism
retinol metabolism
bile Acid Biosynthesis
7
Hydroxysteroid (11-beta) dehydrogenase 2
UDP glycosyltransferase 2 family, polypeptide B7
Hydroxysteroid (17-beta) dehydrogenase 7
Ras homolog enriched in brain
Eukaryotic translation initiation factor 4B
Methylmalonyl Coenzyme A mutase
Sterol carrier protein 2
aldosterone biosynthesis and metabolism
cortisone biosynthesis and metabolism
peroxisomal branched chain fatty acid oxidation
insulin regulation of protein synthesis
8
Phosphoribosyl pyrophosphate synthetase 1-like 1
Placental growth factor, vascular endothelial growth factor -related protein
IMP biosynthesis
VEGF-family signaling
9
Catenin (cadherin-associated protein), alpha 2
Cell division cycle 25C
Retinoblastoma-like 1
SUMO-1 activating enzyme subunit 2
Cyclin E1
cell cycle
cell adhesion
10
Guanine nucleotide binding protein (G protein), gamma 5
Chemokine (C-X-C motif) receptor 4
CXCR4 signaling
11
Baculoviral IAP repeat-containing 5 (survivin)
Von Willebrand factor
blood coagulation
apoptosis and survival
12
Glycosylphosphatidylinositol specific phospholipase D1
Ornithine aminotransferase (gyrate atrophy)
Insulin receptor substrate 1
Sulfotransferase family, cytosolic,2A, DHEA-preferring, member 1
Glutamate dehydrogenase 2
Nuclear receptor subfamily 1, group H, member 4
Acyl-Coenzyme A oxidase 2, branched chain
regulation of lipid metabolism
proline metabolism
13
Glucan (1,4-alpha-), branching enzyme 1
Glycogen synthase 2 (liver)
Cytochrome P450, family 39, subfamily A, polypeptide 1
Lecithin-cholesterol acyltransferase
Leukotriene B4 12-hydroxydehydrogenase
glycogen metabolism
phospholipid metabolism
bile Acid Biosynthesis
14
Activating transcription factor 2
G-protein coupled receptor protein signaling pathway
15
Charcot-Leyden crystal protein
IL2-inducible T-cell kinase
acetylcholine biosynthesis and metabolism
immune response
16
Acetyl-Coenzyme A acyltransferase 2
3-hydroxy-3-methylglutaryl-Coenzyme A synthase 2
Complement component 1, r subcomponent
B-factor, properdin
Complement component 4B, centromeric
Complement component 1, s subcomponent
Clusterin
Ficolin (collagen/fibrinogen domain containing) 3 (Hakata antigen)
classic complement pathway
alternative complement pathway
lectin Induced complement pathway
mitochondrial ketone bodies biosynthesis and metabolism
17
Monoamine oxidase A
Cytochrome P450, family 3, subfamily A, polypeptide 4
Gamma-glutamyl hydrolase
Albumin
vitamin D2 (ergocalciferol) metabolism
estrogen biosynthesis
histamine metabolism
18
Cell division cycle 25A
V-jun sarcoma virus 17 oncogene homolog (avian)
Ring-box 1
HBV-P
Phospholipase A2, group IIA (platelets, synovial fluid)
Fatty acid desaturase 1
Cell division cycle 2, G1 to S and G2 to M
ESR1 regulation of G1/S transition
SCF complex in cell cycle regulation
CD16 signaling in NK cells
beta-adrenergic receptors transactivation of EGFR
19
Caspase 4, apoptosis-related cysteine protease
Sulfotransferase family 1E, estrogen-preferring, member
Choline kinase alpha
Glutamate-ammonia ligase (glutamine synthase)
G protein-coupled receptor 30
phospholipid metabolism
20
Cadherin 15, M-cadherin
CCAAT/enhancer binding protein (C/EBP), beta
Forkhead box O1A
development
apoptosis and survival
cell Adhesion

Table 1
Characteristic genes expressed in CH-B-related HCC.

Genes	Symbol	GenBank ID	Cluster No.	Up- or down-regulated	GO
Placental growth factor, vascular endothelial growth factor-related protein	PGF	NM_002632	8	Up	Angiogenesis
Telomerase-associated protein 1	TEP1	NM_007110	8	Up	Telomere maintenance
Stathmin 1/oncoprotein 18	STMN1	J04991	8	Up	Microtubule depolymerization
SUMO-1 activating enzyme subunit 2	UBA2	NM_005499	9	Up	Protein modification process
Cyclin E1	CCNE1	NM_001238	9	Up	Cell cycle
V-myc myelocytomatosis viral related oncogene	MYCN	NM_005378	9	Up	Regulation of transcription from RNA polymerase II promoter
Glypican 3	GPC3	NM_004484	9	Up	Anatomical structure morphogenesis
Midkine (neurite growth-promoting factor 2)	MDK	NM_002391	9	Up	Cell differentiation
Collagen, type IV, alpha 1	COL4A1	NM_001846	9	Up	Extracellular matrix structural constituent
Gamma-aminobutyric acid (GABA) A receptor	GABRE		11	Up	ion transport
Thrombospondin 2	THBS2	NM_003247	11	Up	Cell adhesion
Transferrin receptor (p90, CD71)	TrF1	AW025110	11	Up	Cellular iron ion homeostasis
Baculoviral IAP repeat containing 5 (Survivin)	BIRC5	NM_001168	11	Up	cytokinesis
Ornithine aminotransferase	OAT	NM_000274	12	Down	Transaminase activity
Insulin receptor substrate 1	IRS1	NM_005544	12	Down	Positive regulation of mesenchymal cell proliferation
Glutamate dehydrogenase 2	GLUD2	NM_012084	12	Down	Cellular amino acid metabolic process
Acyl-CoA oxidase 2	ACOX2	NM_003500	12	Down	Lipid metabolic process
Insulin-like growth factor 2 receptor	IGF-2R	AL353625	13	Down	Transport
Leukocyte cell-derived chemotaxin 2	LECT2, IL-9	AC002428	13	Down	System development
Hydroxysteroid (11-beta) dehydrogenase 1	HSD11B1	NM_181755	13	Down	Lipid metabolic process
Diablo, IAP-binding mitochondrial protein	DIABLO	NM_019887	13	Down	Induction of apoptosis
Cytochrome P450, family 39, subfamily A, polypeptide 1	CYP39A1	NM_016593	13	Down	Bile acid biosynthetic process
N-acetyltransferase 2	NAT-2	NM_000015	13	Down	Metabolic process
Solute carrier family 39 (zinc transporter), member 14	SLC39A14	NM_015359	13	Down	Ion transport
Acetyl-coenzyme A acyltransferase 2	ACAA2	NM_006111	16	Down	Lipid metabolic process

2.4. Framework of gene clusters in relation to hepatocarcinogenesis of CH-B using GGM

We used GGM to examine the relationship between non-cancerous and HCC gene clusters. The partial correlation coefficient matrix (PCCM) generated by GGM is shown in Supplemental Tables H and I. The frame networks of genetic clusters are shown in Fig. 3. The blue lines indicate a negative partial correlation and the black lines indicate a positive partial correlation. Multiple correlations were observed within the non-cancerous and HCC clusters. In addition, some interesting correlations between non-cancerous and HCC clusters were noted. In CH-B (Fig. 3A), non-cancerous cluster No. 3 was up-regulated and correlated with HCC cluster Nos. 8 and 18. Non-cancerous cluster No. 3 was composed of wnt signaling and oxidative stress-related genes, HCC cluster No. 8 was composed of VEGF family signaling-related genes, and HCC cluster No. 18 was composed of estrogen receptor 1 (ESR1) regulation of G1/S transition-related genes. Moreover, non-cancerous cluster No. 16 correlated positively with HCC cluster No. 11 and negatively with HCC cluster No. 18. Non-cancerous cluster No. 16 was composed of cytokine production and apoptosis-related genes, while HCC cluster No. 11 was composed of apoptosis and survival-related genes. The down-regulated non-cancerous cluster No. 13 in CH-B correlated negatively with HCC cluster No. 8. Non-cancerous cluster No. 13 was composed of hepatic functional genes, such as those related to cholesterol metabolism and the TCA cycle.

The correlations between these clusters were further confirmed by examining individual gene interactions with reference to the MetaCore database (Fig. 4A). Eight genes in non-cancerous cluster Nos. 3 and 16 were directly associated with AP1 in HCC cluster No. 18. These genes are related to development and the DNA damage response. In HCC cluster No. 18, many of the cell cycle, development, immune system, and metabolism-related genes were regulated by AP1 [18–20]. In addition, it is interesting to note that the HBV transcript clustered in HCC cluster No. 18 (Fig. 1). The up-regulated HCC cluster No. 11 was associated with AP1 [21]. In addition, the down-regulated HCC cluster No. 13, which included many liver function-related genes, was also associated with AP1 [22,23]. Thus, in CH-B, the DNA damage response might trigger the signaling pathway of HCC, while AP1 in HCC is likely the key regulator of HBV-related HCC.

2.5. Framework of genetic clusters in relation to hepatocarcinogenesis of CH-C using GGM

In CH-C (Fig. 3B), the up-regulated non-cancerous cluster No. 1 correlated negatively with HCC cluster No. 9 and positively with HCC cluster No. 2. Non-cancerous cluster No. 1 was composed of interferon alpha/beta signaling pathway and leukocyte chemotaxis genes. HCC cluster No. 9 was composed of signal transduction and regulation of cell proliferation genes and associated directly with HCC cluster No. 18. HCC cluster Nos. 15 and 18 were composed of development process and wnt signaling pathway genes. HCC cluster Nos. 12 and 14 were composed of immune development, cell adhesion, and defense response genes. These clusters were directly and indirectly associated with HCC cluster No.9. HCC cluster No. 2 was composed of liver function genes, including those for lipid metabolism and iron ion transport. Non-cancerous cluster No. 7, which was composed of immune response, G-protein signaling, and regulation of lipid metabolism genes, correlated positively with HCC cluster No. 18.

Fig. 1. One way hierarchical clustering of 783 differentially expressed genes in CH-B-related HCC.A total of 783 genes were differentially expressed in CH-B-related HCC. Up-regulated genes are shown in red, down-regulated genes are shown in green, and unchanged genes are shown in white.

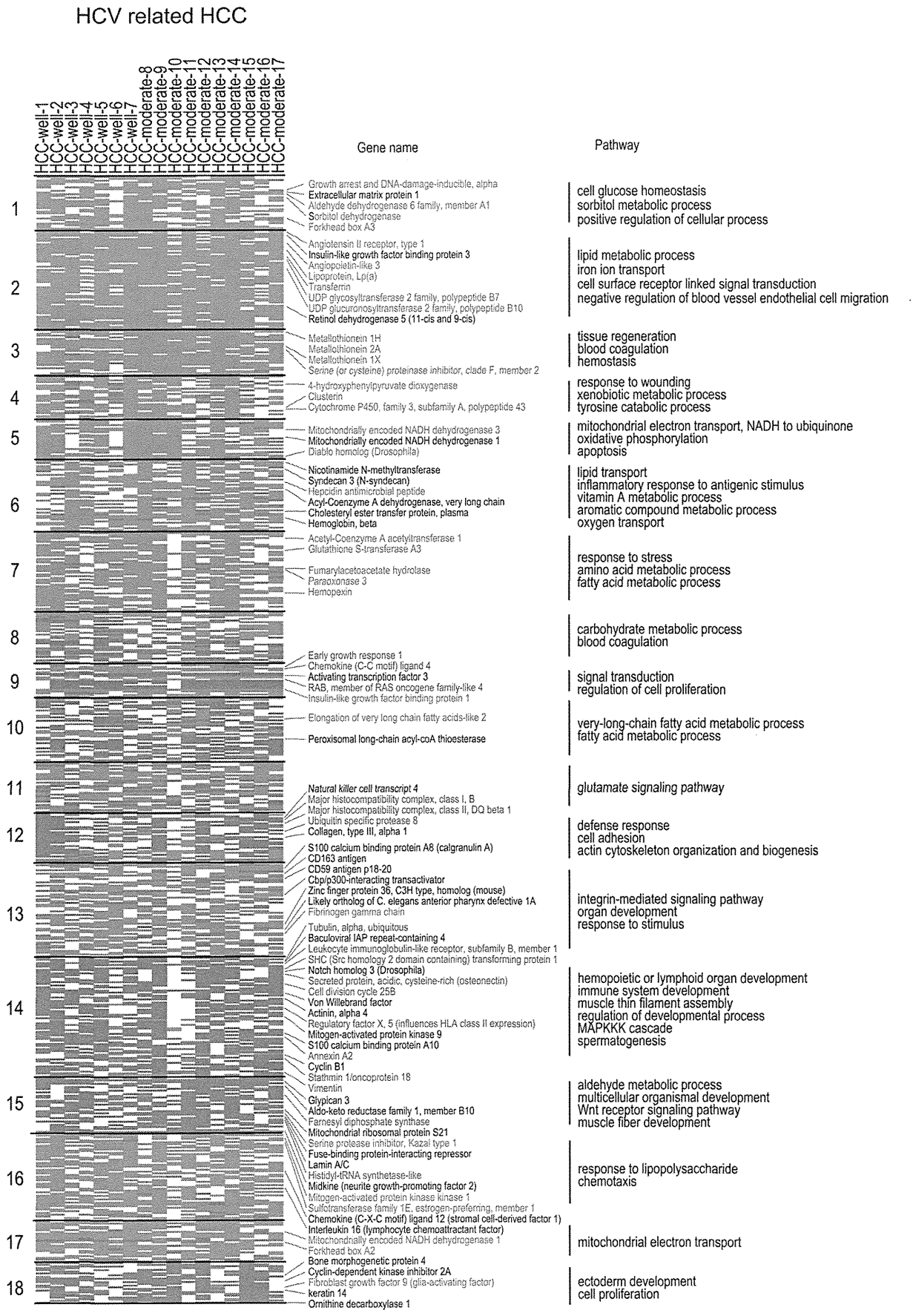
HCV related HCC
HCC-well-1
HCC-well-2
HCC-well-3
HCC-well-4
HCC-well-5
HCC-well-6
HCC-well-7
HCC-moderate-8
HCC-moderate-9
HCC-moderate-10
HCC-moderate-11
HCC-moderate-12
HCC-moderate-13
HCC-moderate-14
HCC-moderate-15
HCC-moderate-16
HCC-moderate-17
Gene name
Pathway
1
Growth arrest and DNA-damage-inducible, alpha
Extracellular matrix protein 1
Aldehyde dehydrogenase 6 family, member A1
Sorbitol dehydrogenase
Forkhead box A3
cell glucose homeostasis
sorbitol metabolic process
positive regulation of cellular process
2
Angiotensin II receptor, type 1
Insulin-like growth factor binding protein 3
Angiopoietin-like 3
Lipoprotein, Lp(a)
Transferrin
UDP glycosyltransferase 2 family, polypeptide B7
UDP glucuronosyltransferase 2 family, polypeptide B10
Retinol dehydrogenase 5 (11-cis and 9-cis)
lipid metabolic process
iron ion transport
cell surface receptor linked signal transduction
negative regulation of blood vessel endothelial cell migration
3
Metallothionein 1H
Metallothionein 2A
Metallothionein 1X
Serine (or cysteine) proteinase inhibitor, clade F, member 2
tissue regeneration
blood coagulation
hemostasis
4
4-hydroxyphenylpyruvate dioxygenase
Clusterin
Cytochrome P450, family 3, subfamily A, polypeptide 43
response to wounding
xenobiotic metabolic process
tyrosine catabolic process
5
Mitochondrially encoded NADH dehydrogenase 3
Mitochondrially encoded NADH dehydrogenase 1
Diablo homolog (Drosophila)
mitochondrial electron transport, NADH to ubiquinone
oxidative phosphorylation
apoptosis
6
Nicotinamide N-methyltransferase
Syndecan 3 (N-syndecan)
Hepcidin antimicrobial peptide
Acyl-Coenzyme A dehydrogenase, very long chain
Cholesteryl ester transfer protein, plasma
Hemoglobin, beta
lipid transport
inflammatory response to antigenic stimulus
vitamin A metabolic process
aromatic compound metabolic process
oxygen transport
7
Acetyl-Coenzyme A acetyltransferase 1
Glutathione S-transferase A3
Fumarylacetoacetate hydrolase
Paraoxonase 3
Hemopexin
response to stress
amino acid metabolic process
fatty acid metabolic process
8
carbohydrate metabolic process
blood coagulation
9
Early growth response 1
Chemokine (C-C motif) ligand 4
Activating transcription factor 3
RAB, member of RAS oncogene family-like 4
Insulin-like growth factor binding protein 1
signal transduction
regulation of cell proliferation
10
Elongation of very long chain fatty acids-like 2
Peroxisomal long-chain acyl-coA thioesterase
very-long-chain fatty acid metabolic process
fatty acid metabolic process
11
Natural killer cell transcript 4
glutamate signaling pathway
12
Major histocompatibility complex, class I, B
Major histocompatibility complex, class II, DQ beta 1
Ubiquitin specific protease 8
Collagen, type III, alpha 1
defense response
cell adhesion
actin cytoskeleton organization and biogenesis
13
S100 calcium binding protein A8 (calgranulin A)
CD163 antigen
CD59 antigen p18-20
Cbp/p300-interacting transactivator
Zinc finger protein 36, C3H type, homolog (mouse)
Likely ortholog of C. elegans anterior pharynx defective 1A
Fibrinogen gamma chain
Tubulin, alpha, ubiquitous
Baculoviral IAP repeat-containing 4
Leukocyte immunoglobulin-like receptor, subfamily B, member 1
SHC (Src homology 2 domain containing) transforming protein 1
integrin-mediated signaling pathway
organ development
response to stimulus
14
Notch homolog 3 (Drosophila)
Secreted protein, acidic, cysteine-rich (osteonectin)
Cell division cycle 25B
Von Willebrand factor
Actinin, alpha 4
Regulatory factor X, 5 (influences HLA class II expression)
Mitogen-activated protein kinase 9
S100 calcium binding protein A10
Annexin A2
Cyclin B1
hemopoietic or lymphoid organ development
immune system development
muscle thin filament assembly
regulation of developmental process
MAPKKK cascade
spermatogenesis
15
Stathmin 1/oncoprotein 18
Vimentin
Glypican 3
Aldo-keto reductase family 1, member B10
Farnesyl diphosphate synthase
Mitochondrial ribosomal protein S21
aldehyde metabolic process
multicellular organismal development
Wnt receptor signaling pathway
muscle fiber development
16
Serine protease inhibitor, Kazal type 1
Fuse-binding protein-interacting repressor
Lamin A/C
Histidyl-tRNA synthetase-like
Midkine (neurite growth-promoting factor 2)
Mitogen-activated protein kinase kinase 1
Sulfotransferase family 1E, estrogen-preferring, member 1
response to lipopolysaccharide
chemotaxis
17
Chemokine (C-X-C motif) ligand 12 (stromal cell-derived factor 1)
Interleukin 16 (lymphocyte chemoattractant factor)
Mitochondrially encoded NADH dehydrogenase 1
Forkhead box A2
mitochondrial electron transport
18
Bone morphogenetic protein 4
Cyclin-dependent kinase inhibitor 2A
Fibroblast growth factor 9 (glia-activating factor)
keratin 14
Ornithine decarboxylase 1
ectoderm development
cell proliferation

Table 2
Characteristic genes expressed in CH-C-related HCC.

Genes	Symbol	GenBank ID	Cluster No.	Up- or down-regulated	GO
Acetyl-coenzyme A acetyltransferase 1	ACAT1	NM_000019	7	Down	Metabolic process
Chemokine (C-C motif) ligand 19	CCL19	NM_006274	12	Up	Immune response
Natural killer cell transcript 4 (Interleukin 32)	IL32	NM_004221	12	Up	Immune response
Major histocompatibility complex, class I, B	HLA-B	NM_005514	12	Up	Immune response
Major histocompatibility complex, class II, DQ beta 1	HLA-DQB1	NM_002123	12	Up	Immune response
Ubiquitin specific protease 8	USP8	NM_005154	12	Up	Cell proliferation
Tubulin, alpha 1b	TUBA1B	NM_006082	14	Up	Microtubule cytoskeleton organization
Actin, alpha 2	ACTA2	NM_001613	14	Up	Vascular smooth muscle contraction
SHC transforming protein 1	SHC1	NM_183001	14	Up	Activation of MAPK activity
Sterile alpha motif domain containing 9	SAMD9	NM_017654	14	Up	Regulation of transcription, dna-dependent
S100 calcium binding protein A10	S100A10	NM_002964	14	Up	Signal transduction
Annexin A2	ANXA2	NM_017654	14	Up	Skeletal system development
Cyclin B1	CCNB1	M25753	14	Up	Cell cycle
Platelet-activating factor acetylhydrolase 1b, 3	PAFAH1B3	D63391	14	Up	Spermatogenesis
Vimentin	VIM	NM_003380	14	Up	Cell motion
Glypican 3	GPC3	NM_004484	15	Up	Anatomical structure morphogenesis
Aldo-keto reductase family 1, member B10	AKR1B10	NM_020299	15	Up	Cellular aldehyde metabolic process
ATP citrate lyase	ACLY	AI819617	15	Up	Lipid biosynthetic process
Farnesyl diphosphate synthase	FDPS	NM_002004	15	Up	Cholesterol biosynthetic process
Serine protease inhibitor, Kazal type 1	SPINK1	NM_003122	15	Up	Protein binding
Bone morphogenetic protein 4	BMP4	D30751	18	Up	Germ cell development
Cyclin-dependent kinase inhibitor 2A	CDKN2A	L27211	18	Up	Cell cycle checkpoint
Fibroblast growth factor 9	FGF9	D14838	18	Up	Signal transduction
Ornithine decarboxylase 1	ODC1	NM_002539	18	Up	Positive regulation of cell proliferation

Analysis of the individual gene interactions (Fig. 4B) showed that a key regulator gene of non-cancerous cluster No. 1, signal transducer and activator of transcription 1 (STAT1), negatively regulated early growth response protein 1 (EGR1) in HCC cluster No. 9 [24]. EGR1 was a key regulator of angiogenesis and fibrogenesis-inducing genes, such as PAI-1 (No. 9), COL1A1, and FAK1 (No. 18) [25–27]. In addition, EGR1 negatively regulated a key regulator of gluconeogenesis, PEPCK (No. 2) [28]. Thus, EGR1 regulated the tissue repair response as well as the metabolic process. In addition to STAT1, phosphatase and tensin homolog (PTEN), in non-cancerous cluster No. 7, negatively regulated FAK1 in HCC cluster No. 18 [29]. FAK1 regulated oncogene SHC (No. 14) and might be involved in the cancer signaling pathway [30,31]. Interestingly, PTEN was associated with Oct-3/4, a regulator of liver differentiation through its target gene C/EBP alpha (No. 3); C/EBP alpha regulated CYP27A1 and CYP3A5 (No. 5). Thus, in CH-C, two antitumor genes, STAT1 and PTEN, were associated with the expression of EGR1 and FAK1, which promote angiogenesis, fibrogenesis, and tumorigenesis in cancerous lesions. Interestingly, the expression of PTEN was related to the metabolic process of CH-C.

2.6. Serial gene expression in non-cancerous gene clusters and the occurrence of HCC

Analysis of the framework of gene clusters in relation to hepatocarcinogenesis by GGM and individual gene interactions revealed several key genes that were associated with hepatocarcinogenesis in non-cancerous clusters. We focused on STAT1 and PTEN in non-cancerous clusters in CH-C and evaluated serial changes of their expression at 2 time points (tumor free and tumor present) in additional 11 patients. The clinical characteristics of these patients at both time points are shown in Supplemental Table J. The expression of STAT1 and its related genes significantly decreased at the time of HCC development compared with the tumor-free time. Similarly, the expression of PTEN significantly decreased when HCC developed compared with the tumor-free time (Supplemental Fig. C2, 3).

3. Discussion

HCC frequently develops in the advanced stage of liver fibrosis. Although gene expression profiling of HCC and the background liver has been studied extensively [32–35], the relationship between the gene expression profiles of different lesions has not been elucidated. In the present study, we utilized GGM [15,16] to analyze the relationship between gene expression in HCC and non-cancerous liver. GGM is widely utilized to study gene association networks [12–14].

We first performed gene expression profiling in CH-B- and CH-C-related HCC. The up- and down-regulated genes were identified by a comparison with a single reference sample of normal liver. There may be some variations in gene expression among normal livers; however, the identified genes were characteristic of HCC and were consistent with previous reports [33,34]. Differences in the signaling pathways between CH-B- and CH-C-related HCC are clearly shown in Figs. 1 and 2 and Supplemental Fig. D. In CH-C-related HCC, immune response- and cytoskeleton-related genes, such as actin, tubulin, and vimentin, were up-regulated, while in CH-B-related HCC, cell matrix interaction genes, such as collagen IV and matrix metalloproteinase, were up-regulated. HBV-X protein reportedly promotes HCC metastasis by the up-regulation of matrix metalloproteinases [36]. The differences in the gene expression profiles between CH-C- and CH-B-related HCC were concordant with those reported previously [34,37].

In the present study, GGM analysis also revealed the interactions of each cluster within HCC as well as within non-cancerous lesions. GGM analysis in CH-B-related HCC showed that 3 up-regulated clusters and 6 down-regulated clusters were associated with each other. In CH-C-related HCC, 4 up-regulated gene clusters and 5 down-regulated gene clusters were associated with each other (Fig. 3). Interestingly, the up-regulated gene clusters were preferentially expressed in CPA in the liver. This prompted us to consider the origin of the HCC cells. Recent reports of immunohistochemical staining of liver tissue using stem cell markers, such as EpCAM and CD133, have suggested the presence of hepatic stem cells in the periportal area [38]. In contrast, many of the down-regulated genes were liver function and metabolism-related genes that were preferentially expressed in CLL in the liver.

Fig. 2. One way hierarchical clustering of 668 differentially expressed genes in CH-B-related HCC.A total of 668 genes were differentially expressed in CH-C-related HCC. Up-regulated genes are shown in red, down-regulated genes are shown in green, and unchanged genes are shown in white (Fig. 2).

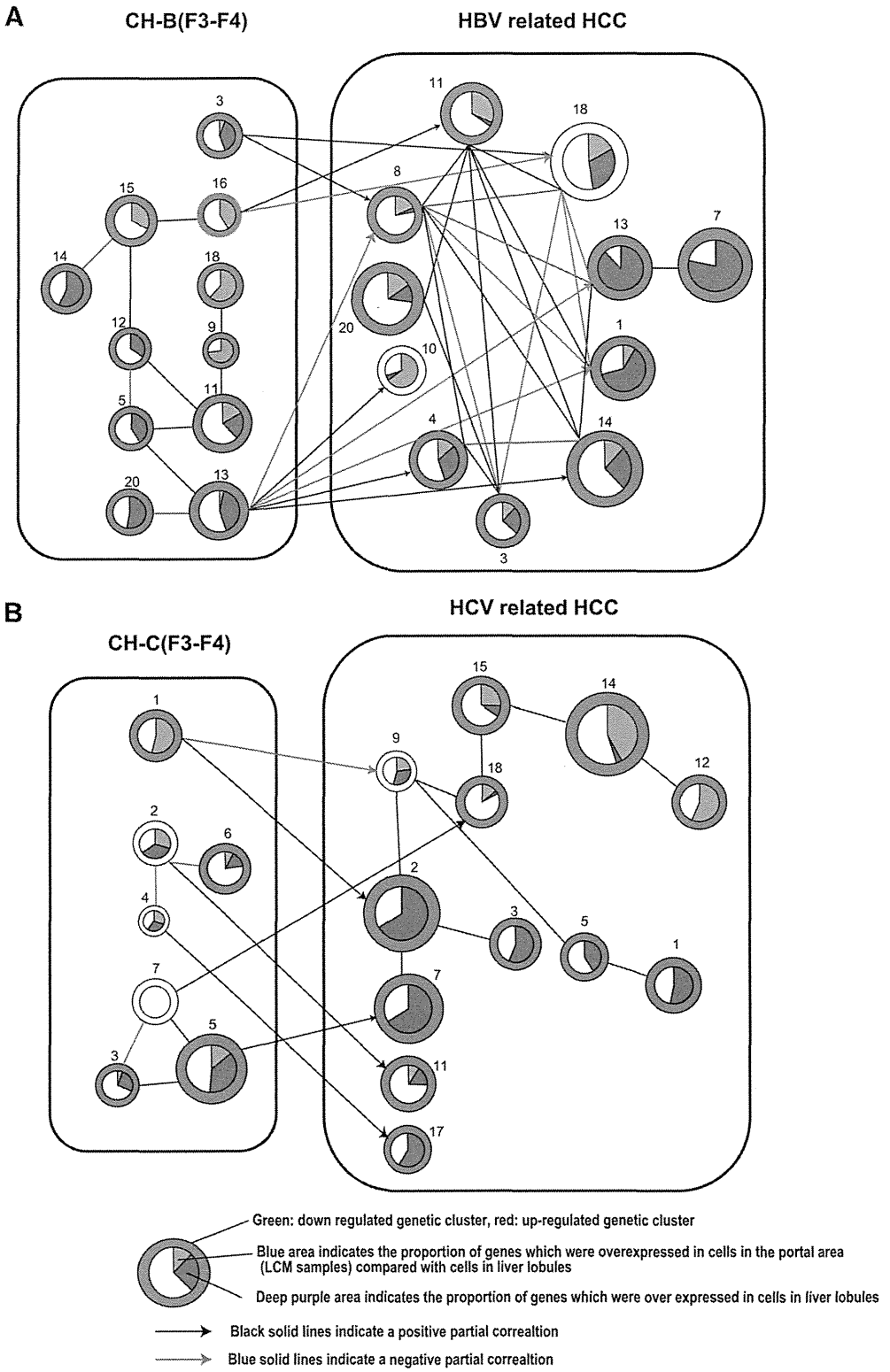

Fig. 3. GGM analysis of each cluster in HCC and non-cancerous lesions. Each cluster in the HCC and non-cancerous lesions was connected according to partial correlation coefficient matrix (PCCM) by GGM algorithms (Supplemental Tables H and I). The blue lines indicate a negative partial correlation and the black lines indicate a positive partial correlation. The size of each cluster reflects the number of clustered genes. The red circles are up-regulated gene clusters, while the green circles are down-regulated gene clusters. Within each cluster, the blue area indicates the proportion of genes that are over-expressed in CPA, while the deep purple area indicates the proportion of genes that are over-expressed in CLL. A; interactions of HBV related clusters. B; interactions of HCV related clusters.

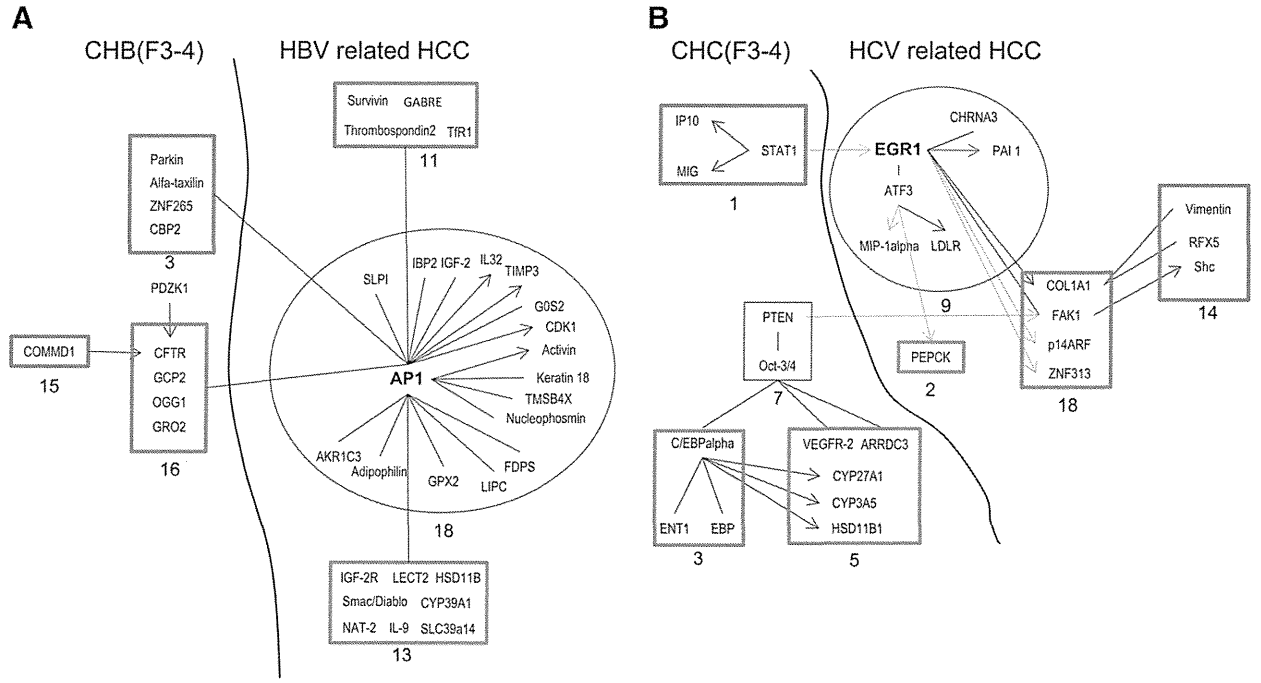

Fig. 4. Individual gene interactions between gene clusters in HCC and non-cancerous lesions. Direct interactions of individual genes among each cluster were confirmed by reference to the MetaCore database. The blue arrows indicate negative regulation, while the black arrows indicate positive regulation. Unspecified interactions are shown with black lines. The red squares are up-regulated gene clusters, while the green squares are down-regulated gene clusters. A; direct interactions of genes in HBV related clusters. B; direct interactions of genes in HCV related clusters.

GGM analysis between the HCC and non-cancerous liver revealed the unique interactions of 2 lesions in this study. In CH-B, up-regulated cluster Nos. 3 and 16, development and DNA damage response gene clusters, regulated HCC cluster Nos. 8, 11, and 18, VEGF-family signaling, apoptosis and survival-related, and ESR1 regulation of G1/S transition-related gene clusters. Down-regulated cluster No. 13, a metabolism-related gene cluster, negatively regulated the up-regulated HCC cluster No. 8. These results suggest that the metabolic status of non-cancerous liver influences the gene expression of HCC. Individual gene interactions with reference to the MetaCore database showed that 8 genes in non-cancerous cluster Nos. 3 and 16 were directly associated with AP1 in HCC cluster No. 18, which regulated the expression of many HCC genes (Fig. 4) [18–23]. Interestingly, the HBV transcript was clustered in HCC cluster No. 18. It has been reported that the HBV transcript enhances AP-1 activation [39,40]. The results suggest a role for the HBV transcript in CH-B-related HCC. Recently, a next generation sequencing approach revealed the frequent integration of HBV in HCC (86.4%), where the putative cancer-related human telomerase reverse transcriptase (hTERT), mixed-lineage leukemia 4, and cyclin E1 genes were located [41]. Although, we could not find the up-regulation of these genes in CH-B-related HCC, HBV genome integration should have important roles for HBV-related hepatocarcinogenesis. A previous report demonstrated that HBx retained the ability to overcome active oncogene RAS-induced senescence by using hTERT, which was introduced into human immortalized primary cells [42].

In CH-C, STAT1 and PTEN signaling in cluster Nos. 1 and 7, respectively, were associated with HCC cluster Nos. 9, 18, and 2, EGR1 signaling, ectodermal development and cell proliferation, lipid metabolism, and iron transport gene clusters. Individual gene interactions with reference to the MetaCore database showed that EGR1 regulates multiple genes in HCC cluster No. 9 as well as genes in up-regulated HCC cluster No. 18 and down-regulated HCC cluster No. 2 (Fig. 4). STAT1 and PTEN in non-cancerous cluster Nos. 1 and 7 exhibited an anti-tumor effect.

STAT1 negatively regulated EGR1 [24] and, interestingly, the expression of PTEN was associated with metabolic-related genes in non-cancerous cluster Nos. 3 and 5 (Fig. 4). PTEN reportedly promotes oxidative phosphorylation, decreases glycolysis, and prevents the metabolic reprogramming of cancer cells [43].

The reduced expression of these antitumor genes in CH-C might increase the expression of EGR1 and FAK1, which promote angiogenesis, fibrogenesis, and tumorigenesis in HCC (Fig. 4). EGR-1 promotes hepatocellular mitotic progression [44], while p53 and PTEN are downstream targets of EGR1. EGR1 might be involved in a negative feedback mechanism of cell cycle progression by inducing p53 and PTEN [45]. Recent reports described the tumorigenic role of EGR1 in the presence of p53 and PTEN mutations [46,47]. Thus, interferon signaling evoked by an innate immune response and the PTEN expression-associated metabolic process (Nos. 3 and 5) will likely regulate the gene expression profile of HCC through EGR1.

It is reported that HBV X protein represses the expression of PTEN by inhibiting the function of p53 [48] and c-Jun promotes cellular survival by suppression of PTEN [49]. In this study, the expression of PTEN was repressed in CH-B (Supplemental Fig. B, CH-B, cluster 21). Possible involvement of HBx, AP-1 and PTEN signaling in HBV-related hepatocarcinogenesis should be explored furthermore.

Recently, Hoshida et al. reported that gene expression profiling of the background liver of patients with HCC predicts their outcome [35]. In their report, gene sets, which correlated with good survival, included many metabolic process genes, such as those of fatty acid, amino acid, and glucose metabolism. In accordance with their results, our findings showed that the possible involvement of metabolic process genes in the background liver might influence gene expression in HCC. In addition, our study revealed the predisposing changes of gene expression in non-cancerous liver that precede the changes of gene expression in HCC. Interestingly, we found that the expression of the anti-tumor genes STAT1 and PTEN was decreased significantly at the onset of HCC compared with the tumor-free time. Therefore, serial analysis of the expression of these genes might be useful for predicting the development of HCC. Several reports have shown that the decreased expression of some chemokines, such as CXCL10, CCL2, and CCL5, is associated with the poor prognosis of resectable HCC [50,51]. In this study, the expression of CXCL10, CXCL6, CXCL9,

and macrophage migration inhibitory factor was decreased at the onset of HCC compared with the tumor-free time (Supplemental Fig. C). It would be worthwhile to examine the expression of these genes in serum samples to predict the development of HCC.

In summary, using a bioinformatics approach, we performed gene expression profiling of HCC and non-cancerous liver, which revealed the predisposing changes of gene expression in HCC. This approach will be useful for the early diagnosis of HCC. Further studies with a larger sample population are needed to confirm our data and to determine possible means for preventing the development of HCC.

4. Materials and methods

4.1. Patients and tissue samples

HCC and non-cancerous liver specimens were obtained from 17 patients with HCV-related HCC and 17 with HBV-related HCC who underwent surgical resection of the liver (Supplemental Tables A and B). For the control normal liver, a surgically obtained tissue sample from a patient who showed no clinical signs of hepatitis was used as described previously [9,10]. The liver tissue was histologically normal, and the patient tested negative for all hepatitis virus markers and had normal levels of serum aminotransferase. HCC and non-cancerous liver tissues were enucleated from resected specimens and frozen immediately in liquid nitrogen for RNA isolation [10]. In a previous study, expression profiling of the liver of 19 patients with CH-B and 18 with CH-C was performed (Table 2) [10]. The other experimental procedures are described in the Supplemental Materials and Methods.

4.2. Microarray analysis

cDNA microarray slides (Liver chip 10 k) were used as described previously [10]. For the selection of genes, we utilized data from the cDNA microarray and hepatic SAGE libraries derived from normal liver, CH-C, CH-C-related HCC, CH-B, and CH-B-related HCC, including 52,149 unique tags. We selected 9614 non-redundant genes that are expressed in diseased and normal liver. The detailed procedures for the preparation of the cDNA microarray slides are described in the Supplemental Material and Methods. RNA isolation, amplification of antisense RNA, labeling, and hybridization were performed according to the protocols described previously [10]. Quantitative assessment of the signals on the slides was performed by scanning on a ScanArray 5000 (General Scanning, Watertown, MA) followed by image analysis using GenePix Pro 4.1 (Axon Instruments, Union City, CA) as described previously [10]. The microarray data have been submitted to the Gene Expression Omnibus (GEO) public database at NCBI (Accession No. GSE41804). The details are also described in the Supplemental Material and Methods.

4.3. Graphical Gaussian modeling data processing

GGM [15,16] enabled us to reveal the gene cluster framework in relation to hepatocellular carcinogenesis of CH-B and CH-C. The procedure included: 1) gene clustering; 2) construction of the PCCM by GGM algorithms; and 3) visualization of the cluster pathway (Supplemental Fig. A).

4.4. Gene selection

To utilize a variety of tissue samples, we first calculated the ratio of gene expression in non-cancerous tissue (36 with CH-B and 35 with CH-C) to that in normal tissue and the ratio of gene expression in HCC tissue (17 with CH-B related HCC and 17 with CH-C related HCC) to that in normal tissue. Then, the expression ratios of non-cancerous and HCC tissues in individual samples were standardized in the two tissues, respectively, by transformation to the Z score (each value was subtracted by the average value and divided by the standard deviation (SD)) such that the mean expression value was 0 and the SD was 1. A gene was regarded as differentially expressed if the Z score was >1 or <-1 ($1 > |AV \pm SD|$). Although the criterion for a differentially expressed gene is usually $|AV \pm 2SD|$, the selection procedure described above is simply designed to gather as many differentially expressed genes as possible, and is suitable for determining the macroscopic relationships between gene systems estimated by cluster analysis. Gene selection from non-HCC samples was performed similarly by avoiding the selected genes in HCC (backward selection). Therefore, a correlation between HCC and non-HCC genes could be obtained as there was no overlap between the genes.

4.5. Clustering with automatic determination of cluster number

In gene profile clustering, the Euclidian distance between Pearson's correlation coefficient of profiles and the unweighted pair group method using the arithmetic average (UPGMA or group average method) were adopted as the metric and the technique, respectively, with reference to previous GGM analysis [15,16]. Note that the present metric and technique were selected to estimate robustly the clusters against the noise of gene expression measurements [15]. In cluster number estimation, the variance inflation factor was adopted as a stopping rule for the hierarchical clustering of expression profiles [15], and the popular cutoff value of 10.0 [52] was adopted as the threshold.

4.6. Graphical Gaussian modeling

The average expression profiles were calculated for the members of each cluster, and the average correlation coefficient matrix between the clusters was calculated. The average correlation coefficient matrix between the clusters was then subjected to GGM as described previously [15,16]. The correlation coefficient can return a false value in the presence of confounding factors. Partial correlation enables replacement of a false-positive correlation with the actual correlation. The PCCM was calculated using GGM (Supplemental Fig. A). All calculations for clustering analysis and GGM were performed via the ASIAN web site (http://eureka.cbrc.jp/asian/index_j.html) [53] and "Auto Net Finder," a commercial desktop version of ASIAN (Infocom Corporation, Shibuya, Tokyo, Japan, http://www.infocom.co.jp/bio/download/).

4.7. Rearrangement of the inferred network

Since the magnitude of the partial correlation coefficient indicates the strength of the association between clusters, the intact network can be rearranged according to the partial correlation coefficient to interpret the association between clusters. The strength of the association can be assigned by a standard test for the partial correlation coefficient. In the present study, the significance level in the t-test was 1% (Supplemental Fig. A).

4.8. Gene ontology of cluster members

Functional ontology enrichment analysis was performed to examine the gene ontology process distribution of each cluster gene using MetaCore™ (Thomson Reuters, New York, NY). Gene ontology was also confirmed by DAVID Bioinformatics Resources 6.7 (http://david.abcc.ncifcrf.gov/) [17].

Supplementary data to this article can be found online at http://dx.doi.org/10.1016/j.ygeno.2013.02.007.

Acknowledgments

The authors thank Nami Nishiyama for excellent technical assistance.

References

[1] R. Siegel, D. Naishadham, A. Jemal, Cancer statistics, 2012, CA Cancer J. Clin. 62 (2012) 10–29.
[2] H. Tsukuma, T. Hiyama, S. Tanaka, M. Nakao, T. Yabuuchi, T. Kitamura, K. Nakanishi, I. Fujimoto, A. Inoue, H. Yamazaki, Risk factors for hepatocellular carcinoma among patients with chronic liver disease, N. Engl. J. Med. 328 (1993) 1797–1801.
[3] A. Arzumanyan, H.M. Reis, M.A. Feitelson, Pathogenic mechanisms in HBV- and HCV-associated hepatocellular carcinoma, Nat. Rev. Cancer 13 (2012) 123–135.
[4] H. Yoshida, Y. Shiratori, M. Moriyama, Y. Arakawa, T. Ide, M. Sata, O. Inoue, M. Yano, M. Tanaka, S. Fujiyama, S. Nishiguchi, T. Kuroki, F. Imazeki, O. Yokosuka, S. Kinoyama, G. Yamada, M. Omata, Interferon therapy reduces the risk for hepatocellular carcinoma: national surveillance program of cirrhotic and noncirrhotic patients with chronic hepatitis C in Japan. IHIT Study Group. Inhibition of hepatocarcinogenesis by interferon therapy, Ann. Intern. Med. 131 (1999) 174–181.
[5] G. Fattovich, T. Stroffolini, I. Zagni, F. Donato, Hepatocellular carcinoma in cirrhosis: incidence and risk factors, Gastroenterology 127 (2004) S35–S50.
[6] A. de La Coste, B. Romagnolo, P. Billuart, C.A. Renard, M.A. Buendia, O. Soubrane, M. Fabre, J. Chelly, C. Beldjord, A. Kahn, C. Perret, Somatic mutations of the beta-catenin gene are frequent in mouse and human hepatocellular carcinomas, Proc. Natl. Acad. Sci. U. S. A. 95 (1998) 8847–8851.
[7] D.F. Calvisi, S. Ladu, A. Gorden, M. Farina, E.A. Conner, J.S. Lee, V.M. Factor, S.S. Thorgeirsson, Ubiquitous activation of Ras and Jak/Stat pathways in human HCC, Gastroenterology 130 (2006) 1117–1128.
[8] G.H. Thoresen, T.K. Guren, D. Sandnes, M. Peak, L. Agius, T. Christoffersen, Response to transforming growth factor alpha (TGFalpha) and epidermal growth factor (EGF) in hepatocytes: lower EGF receptor affinity of TGFalpha is associated with more sustained activation of p42/p44 mitogen-activated protein kinase and greater efficacy in stimulation of DNA synthesis, J. Cell. Physiol. 175 (1998) 10–18.
[9] M. Honda, S. Kaneko, H. Kawai, Y. Shirota, K. Kobayashi, Differential gene expression between chronic hepatitis B and C hepatic lesion, Gastroenterology 120 (2001) 955–966.
[10] M. Honda, T. Yamashita, T. Ueda, H. Takatori, R. Nishino, S. Kaneko, Different signaling pathways in the livers of patients with chronic hepatitis B or chronic hepatitis C, Hepatology 44 (2006) 1122–1138.
[11] M. Honda, M. Nakamura, M. Tateno, A. Sakai, T. Shimakami, T. Shirasaki, T. Yamashita, K. Arai, T. Yamashita, Y. Sakai, S. Kaneko, Differential interferon signaling in liver lobule and portal area cells under treatment for chronic hepatitis C, J. Hepatol. 53 (2010) 817–826.
[12] H. Kishino, P.J. Waddell, Correspondence analysis of genes and tissue types and finding genetic links from microarray data, Genome Inform. Ser. Workshop Genome Inform. 11 (2000) 83–95.
[13] P.J. Waddell, H. Kishino, Cluster inference methods and graphical models evaluated on NCI60 microarray gene expression data, Genome Inform. Ser. Workshop Genome Inform. 11 (2000) 129–140.
[14] J. Krumsiek, K. Suhre, T. Illig, J. Adamski, F.J. Theis, Gaussian graphical modeling reconstructs pathway reactions from high-throughput metabolomics data, BMC Syst. Biol. 5 (2011) 21.
[15] H. Toh, K. Horimoto, Inference of a genetic network by a combined approach of cluster analysis and graphical Gaussian modeling, Bioinformatics 18 (2002) 287–297.
[16] S. Aburatani, F. Sun, S. Saito, M. Honda, S. Kaneko, K. Horimoto, Gene systems network inferred from expression profiles in hepatocellular carcinogenesis by graphical Gaussian model, EURASIP J. Bioinform. Syst. Biol. (2007) 47214.
[17] W. Huang da, B.T. Sherman, Q. Tan, J. Kir, D. Liu, D. Bryant, Y. Guo, R. Stephens, M.W. Baseler, H.C. Lane, R.A. Lempicki, DAVID bioinformatics resources: expanded annotation database and novel algorithms to better extract biology from large gene lists, Nucleic Acids Res. 35 (2007) W169–W175.
[18] L. Russell, D.R. Forsdyke, A human putative lymphocyte G0/G1 switch gene containing a CpG-rich island encodes a small basic protein with the potential to be phosphorylated, DNA Cell Biol. 10 (1991) 581–591.
[19] L. Zhong, J. Ou, U. Barkai, J.F. Mao, J. Frasor, G. Gibori, Molecular cloning and characterization of the rat ovarian 20 alpha-hydroxysteroid dehydrogenase gene, Biochem. Biophys. Res. Commun. 249 (1998) 797–803.
[20] K.M. Mani, C. Lefebvre, K. Wang, W.K. Lim, K. Basso, R. Dalla-Favera, A. Califano, A systems biology approach to prediction of oncogenes and molecular perturbation targets in B-cell lymphomas, Mol. Syst. Biol. 4 (2008) 169.
[21] H.K. Kwon, J.S. Hwang, J.S. So, C.G. Lee, A. Sahoo, J.H. Ryu, W.K. Jeon, B.S. Ko, C.R. Im, S.H. Lee, Z.Y. Park, S.H. Im, Cinnamon extract induces tumor cell death through inhibition of NFkappaB and AP1, BMC Cancer 10 (2010) 392.
[22] K.R. Mitchell, D. Warshawsky, Xenobiotic inducible regions of the human arylamine N-acetyltransferase 1 and 2 genes, Toxicol. Lett. 139 (2003) 11–23.
[23] D. Bottomly, S.L. Kyler, S.K. McWeeney, G.S. Yochum, Identification of {beta}-catenin binding regions in colon cancer cells using ChIP-Seq, Nucleic Acids Res. 38 (2010) 5735–5745.
[24] J.L. Ingram, A. Antao-Menezes, J.B. Mangum, O. Lyght, P.J. Lee, J.A. Elias, J.C. Bonner, Opposing actions of Stat1 and Stat6 on IL-13-induced up-regulation of early growth response-1 and platelet-derived growth factor ligands in pulmonary fibroblasts, J. Immunol. 177 (2006) 4141–4148.
[25] H. Liao, M.C. Hyman, D.A. Lawrence, D.J. Pinsky, Molecular regulation of the PAI-1 gene by hypoxia: contributions of Egr-1, HIF-1alpha, and C/EBPalpha, FASEB J. 21 (2007) 935–949.
[26] V. Lejard, F. Blais, M.J. Guerquin, A. Bonnet, M.A. Bonnin, E. Havis, M. Malbouyres, C.B. Bidaud, G. Maro, P. Gilardi-Hebenstreit, J. Rossert, F. Ruggiero, D. Duprez, EGR1 and EGR2 involvement in vertebrate tendon differentiation, J. Biol. Chem. 286 (2011) 5855–5867.
[27] V. Golubovskaya, A. Kaur, W. Cance, Cloning and characterization of the promoter region of human focal adhesion kinase gene: nuclear factor kappa B and p53 binding sites, Biochim. Biophys. Acta 1678 (2004) 111–125.
[28] S.P. Berasi, C. Huard, D. Li, H.H. Shih, Y. Sun, W. Zhong, J.E. Paulsen, E.L. Brown, R.E. Gimeno, R.V. Martinez, Inhibition of gluconeogenesis through transcriptional activation of EGR1 and DUSP4 by AMP-activated kinase, J. Biol. Chem. 281 (2006) 27167–27177.
[29] J. Gu, M. Tamura, R. Pankov, E.H. Danen, T. Takino, K. Matsumoto, K.M. Yamada, Shc and FAK differentially regulate cell motility and directionality modulated by PTEN, J. Cell Biol. 146 (1999) 389–403.
[30] J.F. Rual, K. Venkatesan, T. Hao, T. Hirozane-Kishikawa, A. Dricot, N. Li, G.F. Berriz, F.D. Gibbons, M. Dreze, N. Ayivi-Guedehoussou, N. Klitgord, C. Simon, M. Boxem, S. Milstein, J. Rosenberg, D.S. Goldberg, L.V. Zhang, S.L. Wong, G. Franklin, S. Li, J.S. Albala, J. Lim, C. Fraughton, E. Llamosas, S. Cevik, C. Bex, P. Lamesch, R.S. Sikorski, J. Vandenhaute, H.Y. Zoghbi, A. Smolyar, S. Bosak, R. Sequerra, L. Doucette-Stamm, M.E. Cusick, D.E. Hill, F.P. Roth, M. Vidal, Towards a proteome-scale map of the human protein–protein interaction network, Nature 437 (2005) 1173–1178.
[31] T.P. Hecker, J.R. Grammer, G.Y. Gillespie, J. Stewart, C.L. Gladson, Focal adhesion kinase enhances signaling through the Shc/extracellular signal-regulated kinase pathway in anaplastic astrocytoma tumor biopsy samples, Cancer Res. 62 (2002) 2699–2707.
[32] H. Okabe, S. Satoh, T. Kato, O. Kitahara, R. Yanagawa, Y. Yamaoka, T. Tsunoda, Y. Furukawa, Y. Nakamura, Genome-wide analysis of gene expression in human hepatocellular carcinomas using cDNA microarray: identification of genes involved in viral carcinogenesis and tumor progression, Cancer Res. 61 (2001) 2129–2137.
[33] Y. Hippo, K. Watanabe, A. Watanabe, Y. Midorikawa, S. Yamamoto, S. Ihara, S. Tokita, H. Iwanari, Y. Ito, K. Nakano, J. Nezu, H. Tsunoda, T. Yoshino, I. Ohizumi, M. Tsuchiya, S. Ohnishi, M. Makuuchi, T. Hamakubo, T. Kodama, H. Aburatani, Identification of soluble NH2-terminal fragment of glypican-3 as a serological marker for early-stage hepatocellular carcinoma, Cancer Res. 64 (2004) 2418–2423.
[34] Y. Shirota, S. Kaneko, M. Honda, H.F. Kawai, K. Kobayashi, Identification of differentially expressed genes in hepatocellular carcinoma with cDNA microarrays, Hepatology 33 (2001) 832–840.
[35] Y. Hoshida, A. Villanueva, M. Kobayashi, J. Peix, D.Y. Chiang, A. Camargo, S. Gupta, J. Moore, M.J. Wrobel, J. Lerner, M. Reich, J.A. Chan, J.N. Glickman, K. Ikeda, M. Hashimoto, G. Watanabe, M.G. Daidone, S. Roayaie, M. Schwartz, S. Thung, H.B. Salvesen, S. Gabriel, V. Mazzaferro, J. Bruix, S.L. Friedman, H. Kumada, J.M. Llovet, T.R. Golub, Gene expression in fixed tissues and outcome in hepatocellular carcinoma, N. Engl. J. Med. 359 (2008) 1995–2004.
[36] L. Xia, W. Huang, D. Tian, H. Zhu, Y. Zhang, H. Hu, D. Fan, Y. Nie, K. Wu, Upregulated FoxM1 expression induced by hepatitis B virus X protein promotes tumor metastasis and indicates poor prognosis in hepatitis B virus-related hepatocellular carcinoma, J. Hepatol. 57 (2012) 600–612.
[37] S. Ura, M. Honda, T. Yamashita, T. Ueda, H. Takatori, R. Nishino, H. Sunakozaka, Y. Sakai, K. Horimoto, S. Kaneko, Differential microRNA expression between hepatitis B and hepatitis C leading disease progression to hepatocellular carcinoma, Hepatology 49 (2009) 1098–1112.
[38] R. Turner, O. Lozoya, Y. Wang, V. Cardinale, E. Gaudio, G. Alpini, G. Mendel, E. Wauthier, C. Barbier, D. Alvaro, L.M. Reid, Human hepatic stem cell and maturational liver lineage biology, Hepatology 53 (2011) 1035–1045.
[39] K.M. Sze, G.K. Chu, J.M. Lee, I.O. Ng, C-terminal truncated HBx is associated with metastasis and enhances invasiveness via C-Jun / MMP10 activation in hepatocellular carcinoma, Hepatology (2012).
[40] Y. Tanaka, F. Kanai, T. Ichimura, K. Tateishi, Y. Asaoka, B. Guleng, A. Jazag, M. Ohta, J. Imamura, T. Ikenoue, H. Ijichi, T. Kawabe, T. Isobe, M. Omata, The hepatitis B virus X protein enhances AP-1 activation through interaction with Jab1, Oncogene 25 (2006) 633–642.
[41] W.K. Sung, H. Zheng, S. Li, R. Chen, X. Liu, Y. Li, N.P. Lee, W.H. Lee, P.N. Ariyaratne, C. Tennakoon, F.H. Mulawadi, K.F. Wong, A.M. Liu, R.T. Poon, S.T. Fan, K.L. Chan, Z. Gong, Y. Hu, Z. Lin, G. Wang, Q. Zhang, T.D. Barber, W.C. Chou, A. Aggarwal, K. Hao, W. Zhou, C. Zhang, J. Hardwick, C. Buser, J. Xu, Z. Kan, H. Dai, M. Mao, C. Reinhard, J. Wang, J.M. Luk, Genome-wide survey of recurrent HBV integration in hepatocellular carcinoma, Nat. Genet. 44 (2012) 765–769.
[42] N. Oishi, K. Shilagardi, Y. Nakamoto, M. Honda, S. Kaneko, S. Murakami, Hepatitis B virus X protein overcomes oncogenic RAS-induced senescence in human immortalized cells, Cancer Sci. 98 (2007) 1540–1548.
[43] A. Ortega-Molina, M. Serrano, PTEN in cancer, metabolism, and aging, Trends Endocrinol. Metab. (2012).
[44] Y. Liao, O.N. Shikapwashya, E. Shteyer, B.K. Dieckgraefe, P.W. Hruz, D.A. Rudnick, Delayed hepatocellular mitotic progression and impaired liver regeneration in early growth response-1-deficient mice, J. Biol. Chem. 279 (2004) 43107–43116.
[45] Y. Zwang, A. Sas-Chen, Y. Drier, T. Shay, R. Avraham, M. Lauriola, E. Shema, E. Lidor-Nili, J. Jacob-Hirsch, N. Amariglio, Y. Lu, G.B. Mills, G. Rechavi, M. Oren, E. Domany, Y. Yarden, Two phases of mitogenic signaling unveil roles for p53 and EGR1 in elimination of inconsistent growth signals, Mol. Cell 42 (2011) 524–535.
[46] J. Yu, S.S. Zhang, K. Saito, S. Williams, Y. Arimura, Y. Ma, Y. Ke, V. Baron, D. Mercola, G.S. Feng, E. Adamson, T. Mustelin, PTEN regulation by Akt-EGR1-ARF-PTEN axis, EMBO J. 28 (2009) 21–33.
[47] D. Lu, C. Han, T. Wu, Microsomal prostaglandin E synthase-1 promotes hepatocarcinogenesis through activation of a novel EGR1/beta-catenin signaling axis, Oncogene 31 (2012) 842–857.
[48] T.W. Chung, Y.C. Lee, J.H. Ko, C.H. Kim, Hepatitis B Virus X protein modulates the expression of PTEN by inhibiting the function of p53, a transcriptional activator in liver cells, Cancer Res. 63 (2003) 3453–3458.
[49] K. Hettinger, F. Vikhanskaya, M.K. Poh, M.K. Lee, I. de Belle, J.T. Zhang, S.A. Reddy, K. Sabapathy, c-Jun promotes cellular survival by suppression of PTEN, Cell Death Differ. 14 (2007) 218–229.

[50] V. Chew, C. Tow, M. Teo, H.L. Wong, J. Chan, A. Gehring, M. Loh, A. Bolze, R. Quek, V.K. Lee, K.H. Lee, J.P. Abastado, H.C. Toh, A. Nardin, Inflammatory tumour microenvironment is associated with superior survival in hepatocellular carcinoma patients, J. Hepatol. 52 (2010) 370–379.
[51] V. Chew, J. Chen, D. Lee, E. Loh, J. Lee, K.H. Lim, A. Weber, K. Slankamenac, R.T. Poon, H. Yang, L.L. Ooi, H.C. Toh, M. Heikenwalder, I.O. Ng, A. Nardin, J.P. Abastado, Chemokine-driven lymphocyte infiltration: an early intratumoural event determining long-term survival in resectable hepatocellular carcinoma, Gut 61 (2012) 427–438.
[52] R.J. Freund, W.J. Wilson, Regression analysis : statistical modeling of a response variable, Academic Press, San Diego, 1998.
[53] S. Aburatani, K. Goto, S. Saito, H. Toh, K. Horimoto, ASIAN: a web server for inferring a regulatory network framework from gene expression profiles, Nucleic Acids Res. 33 (2005) W659–W664.

HEPATOLOGY
Official Journal of the American Association for the Study of Liver Diseases

Discrete Nature of EpCAM$^+$ and CD90$^+$ Cancer Stem Cells in Human Hepatocellular Carcinoma

Taro Yamashita,[1] Masao Honda,[1] Yasunari Nakamoto,[1] Masayo Baba,[1] Kouki Nio,[1] Yasumasa Hara,[1] Sha Sha Zeng,[1] Takehiro Hayashi,[1] Mitsumasa Kondo,[1] Hajime Takatori,[1] Tatsuya Yamashita,[1] Eishiro Mizukoshi,[1] Hiroko Ikeda,[1] Yoh Zen,[1] Hiroyuki Takamura,[1] Xin Wei Wang,[2] and Shuichi Kaneko[1]

Recent evidence suggests that hepatocellular carcinoma (HCC) is organized by a subset of cells with stem cell features (cancer stem cells; CSCs). CSCs are considered a pivotal target for the eradication of cancer, and liver CSCs have been identified by the use of various stem cell markers. However, little information is known about the expression patterns and characteristics of marker-positive CSCs, hampering the development of personalized CSC-targeted therapy. Here, we show that CSC markers EpCAM and CD90 are independently expressed in liver cancer. In primary HCC, EpCAM$^+$ and CD90$^+$ cells resided distinctively, and gene-expression analysis of sorted cells suggested that EpCAM$^+$ cells had features of epithelial cells, whereas CD90$^+$ cells had those of vascular endothelial cells. Clinicopathological analysis indicated that the presence of EpCAM$^+$ cells was associated with poorly differentiated morphology and high serum alpha-fetoprotein (AFP), whereas the presence of CD90$^+$ cells was associated with a high incidence of distant organ metastasis. Serial xenotransplantation of EpCAM$^+$/CD90$^+$ cells from primary HCCs in immunedeficient mice revealed rapid growth of EpCAM$^+$ cells in the subcutaneous lesion and a highly metastatic capacity of CD90$^+$ cells in the lung. In cell lines, CD90$^+$ cells showed abundant expression of c-Kit and *in vitro* chemosensitivity to imatinib mesylate. Furthermore, CD90$^+$ cells enhanced the motility of EpCAM$^+$ cells when cocultured *in vitro* through the activation of transforming growth factor beta (TGF-β) signaling, whereas imatinib mesylate suppressed *TGFB1* expression in CD90$^+$ cells as well as CD90$^+$ cell-induced motility of EpCAM$^+$ cells. *Conclusion*: Our data suggest the discrete nature and potential interaction of EpCAM$^+$ and CD90$^+$ CSCs with specific gene-expression patterns and chemosensitivity to molecular targeted therapy. The presence of distinct CSCs may determine the clinical outcome of HCC. (HEPATOLOGY 2013;57:1484-1497)

The cancer stem cell (CSC) hypothesis, which suggests that a subset of cells bearing stem-cell–like features is indispensable for tumor development, has recently been put forward subsequent to advances in molecular and stem cell biology. Liver cancer, including hepatocellular carcinoma (HCC), is a leading cause of cancer death worldwide.[1] Recent studies have shown the existence of CSCs in liver cancer cell lines and primary HCC specimens using various stem cell markers.[2-7] Independently, we have identified novel HCC subtypes defined by the hepatic stem/progenitor cell markers,

Abbreviations: 5-FU, fluorouracil; Abs, antibodies; AFP, alpha-fetoprotein; CK-19, cytokeratin-19; CSC, cancer stem cell; DNs, dysplastic nodules; EMT, epithelial mesenchymal transition; EpCAM; epithelial cell adhesion molecule; FACS, fluorescent-activated cell sorting; HBV, hepatitis B virus; HCC, hepatocellular carcinoma; HCV, hepatitis C virus; HSCs, hepatic stem cells; IF, immunofluorescence; IHC, immunohistochemistry; IR, immunoreactivity; MDS, multidimensional scaling; NBNC, non-B, non-C hepatitis; NOD/SCID, nonobese diabetic, severe combined immunodeficient; NT, nontumor; OV-1, ovalbumin 1; qPCR, quantitative real-time polymerase chain reaction; SC, subcutaneous; Smad3, Mothers against decapentaplegic homolog 3; TECs, tumor epithelial cells; TGF-β, transforming growth factor beta; T/N, tumor/nontumor; VECs, vascular endothelial cells; VM, vasculogenic mimicry; VEGFR, vascular endothelial growth factor receptor.

From the [1]Liver Center, Kanazawa University Hospital, Kanazawa, Ishikawa, Japan; and [2]Laboratory of Human Carcinogenesis, Center for Cancer Research, National Cancer Institute, Bethesda, MD.

Received July 9, 2012; revised October 22, 2012; accepted November 6, 2012.

This study was supported by a Grant-in-Aid from the Ministry of Education, Culture, Sports, Science, and Technology of Japan (23590967), a grant from the Japanese Society of Gastroenterology, a grant from the Ministry of Health, Labor, and Welfare, and a grant from the National Cancer Center Research and Development Fund (23-B-5) of Japan. X.W.W. is supported by the Intramural Research Program of the Center for Cancer Research, U.S. National Cancer Institute.

epithelial cell adhesion molecule (EpCAM) and alpha-fetoprotein (AFP), which correlate with distinct gene-expression signatures and prognosis.[8,9] $EpCAM^+$ HCC cells isolated from primary HCC and cell lines show CSC features, including tumorigenicity, invasiveness, and resistance to fluorouracil (5-FU).[10] Similarly, other groups have shown that $CD133^+$, $CD90^+$, and $CD13^+$ HCC cells are also CSCs, and that EpCAM, CD90, and CD133 are the only markers confirmed to enrich CSCs from primary HCCs thus far.[3-5,10]

Although $EpCAM^+$, $CD90^+$, and $CD133^+$ cells show CSC features, such as high tumorigenicity, an invasive nature, and resistance to chemo- and radiation therapy, it remains unclear whether these cells represent an identical HCC population and whether they share similar or distinct characteristics. In this study, we used fluorescent-activated cell sorting (FACS), microarray, and immunohistochemistry (IHC) techniques to investigate the expression patterns of the representative liver CSC markers CD133, CD90, and EpCAM in a total of 340 HCC cases and 7 cases of mesenchymal liver tumors. We further explored gene- and protein-expression patterns as well as tumorigenic capacity of sorted cells isolated from 15 primary HCCs and 7 liver cancer cell lines in an attempt to identify the molecular portraits of each cell type.

Materials and Methods

Clinical Specimens. HCC samples were obtained with informed consent from patients who had undergone radical resection at the Liver Center in Kanazawa University Hospital (Kanazawa, Japan), and tissue acquisition procedures were approved by the ethics committee of Kanazawa University. A total of 102 formalin-fixed and paraffin-embedded HCC samples, obtained from 2001 to 2007, were used for IHC analyses. Fifteen fresh HCC samples were obtained between 2008 and 2012 from surgically resected specimens and an autopsy specimen and were used immediately to prepare single-cell suspensions and xenotransplantation (Table 1). Seven hepatic stromal tumors (three cavernous hemangioma, two hemangioendothelioma, and two angiomyolipoma) were formalin fixed and paraffin embedded and used for IHC analyses.

Table 1. Clinicopathological Characteristics of HCC Cases Used for Xenotransplantation

ID	Age/ Sex	Etiology	Tumor Size (cm)	Histological Grade	AFP (ng/mL)	DCP (IU/mL)
P1	77/M	Alcohol	12.0	Moderate	198	322
P2	61/F	NBNC	11.0	Moderate	12	3,291
P3	66/M	NBNC	2.2	Moderate	13	45
P4	65/M	HCV	4.2	Poor	13,700	25,977
P5	52/M	HBV	6.0	Moderate	29,830	1,177
P6	60/M	HCV	2.7	Poor	249	185
P7	79/F	HBV	4.0	Poor	46,410	384
P8	77/F	NBNC	5.5	Moderate	17,590	562
P9	71/M	Alcohol	7.0	Poor	3,814	607
P10	51/M	HBV	2.2	Well	<10	21
P11	71/M	Alcohol	2.1	Well	<10	11
P12	60/M	HBV	10.8	Poor	323	2,359
P13	66/M	HCV	2.8	Moderate	11	29
P14	71/M	HCV	7.2	Moderate	235,700	375,080
P15	75/M	HBV	5.5	Poor	<10	97

Abbreviation: DCP, des-gamma-carboxy prothrombin.

Additional details of experimental procedures are available in the Supporting Information.

Results

EpCAM, CD133, and CD90 Expression in HCC. We first evaluated the frequencies of three representative CSC markers ($EpCAM^+$, $CD90^+$, and $CD133^+$ cells) in 12 fresh primary HCC cases surgically resected by FACS (representative data shown in Fig. 1A). Clinicopathological characteristics of primary HCC cases are shown in Table 1. We noted that frequency of $EpCAM^+$, $CD90^+$, and $CD133^+$ cells varied between individuals. Abundant $CD90^+$ (7.0%), but almost no $EpCAM^+$, cells (0.06%, comparable to the isotype control) were detected in P2, whereas few $CD90^+$ (0.6%), but abundant $EpCAM^+$, cells (17.5%) were detected in P4. Very small populations of $EpCAM^+$ (0.09%), $CD90^+$ (0.04%), and $CD133^+$ cells (0.05%) were found in P12, but they were almost nonexistent in P8, except for $CD90^+$ cells (0.08%) (Fig. 1A). We further evaluated the expression of EpCAM, CD90, and CD133 in xenografts obtained from surgically resected samples (P13 and P15) and an autopsy sample (P14). As a whole, compared to the isotype control, 7 of 15 HCCs contained definite $EpCAM^+$ cells (46.7%), whereas only 3 HCCs

Address reprint requests to: Taro Yamashita, M.D., Ph.D., Department of General Medicine, Kanazawa University Hospital, 13-1 Takara-Machi, Kanazawa, Ishikawa 920-8641, Japan. E-mail: taroy@m-kanazawa.jp; fax: +81-76-234-4250.

View this article online at wileyonlinelibrary.com.
DOI 10.1002/hep.26168
Potential conflict of interest: Nothing to report.
Additional Supporting Information may be found in the online version of this article.

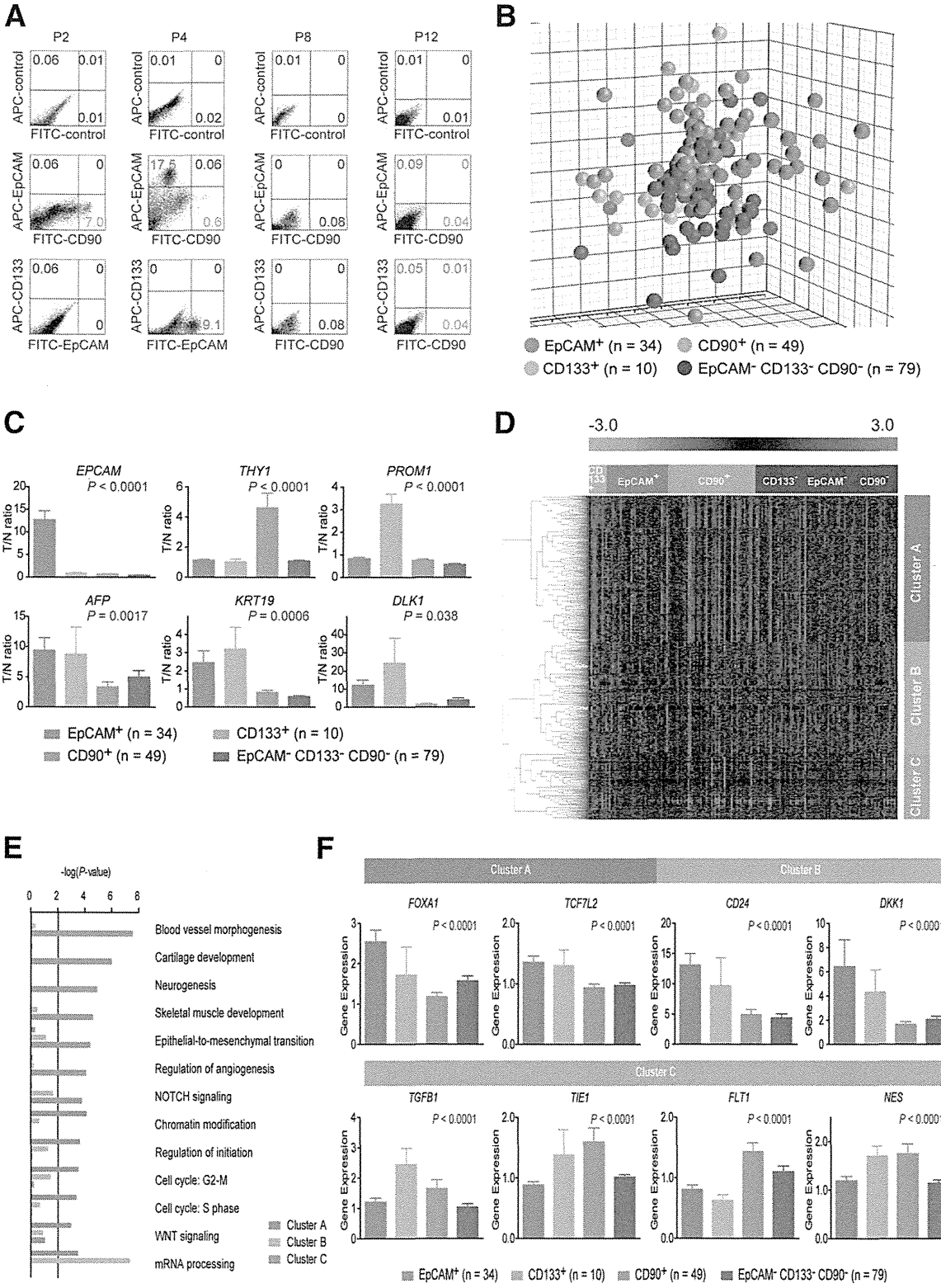

Fig. 1. Gene-expression profiles of CSC marker-positive HCCs. (A) FACS analysis of primary HCCs stained with fluorescent-labeled Abs against EpCAM, CD90, or CD133. (B) Multidimensional scaling analysis of 172 HCC cases characterized by the expression patterns of EpCAM, CD133, and CD90. Red, $EpCAM^{+}$ $CD90^{-}$ $CD133^{-}$ (n = 34); orange, $EpCAM^{-}$ $CD90^{-}$ $CD133^{+}$ (n = 10); light blue, $EpCAM^{-}$ $CD90^{+}$ $CD133^{-}$ (n = 49); blue, $EpCAM^{-}$ $CD90^{-}$ $CD133^{-}$ (n = 79). HCC specimens were clustered in specific groups with statistical significance ($P < 0.001$). (C) Expression patterns of well-known hepatic stem/progenitor markers in each HCC subtype, as analyzed by microarray. Red bar, $EpCAM^{+}$; orange bar, $CD133^{+}$; light blue bar, $CD90^{+}$; blue bar, $EpCAM^{-}$ $CD90^{-}$ $CD133^{-}$. (D) Hierarchical cluster analysis based on 1,561 EpCAM/CD90/CD133-coregulated genes in 172 HCC cases. Each cell in the matrix represents the expression level of a gene in an individual sample. Red and green cells depict high and low expression levels, respectively, as indicated by the scale bar. (E) Pathway analysis of EpCAM/CD90/CD133-coregulated genes. Canonical signaling pathways activated in cluster A (red bar), cluster B (orange bar), or cluster C (light blue bar) with statistical significance ($P < 0.01$) are shown. (F) Expression patterns of representative genes differentially expressed in EpCAM/CD90/CD133 HCC subtypes. Red bar, $EpCAM^{+}$; orange bar, $CD133^{+}$; light blue bar, $CD90^{+}$; blue bar, $EpCAM^{-}$ $CD133^{-}$ $CD90^{-}$.